INVESTIGATION OF HIP JOINT KINEMATICS FOR DAILY LIFE ACTIVITIES

A Thesis Submitted to
The Graduate School of Engineering and Science of
İzmir Institute of Technology
In Partial Fulfillments of the Requirements for the Degree of

MASTER OF SCIENCE

in Mechanical Engineering

by
Merve TUNA

December 2022
İZMİR

ACKNOWLEDGEMENTS

I would like to thank my supervisor Dr. Şenay Mihçin for her endless support, valuable advice, and guidance during my thesis studies. It has been a great chance to take a part in a comprehensive project that improves me in countless ways.

I would like to thank Ahmet Mert Şahin who is a member of Biomechanics and Motion Capture Systems Laboratory for his valuable supports regardless of time and date.

I'm also grateful to members of Alpmed Healthcare Technologies and Solutions for their support in any time I required.

I would like to express my gratitude to the physiotherapists took part on the project for providing trainings to enlighten me about critical points of the research area.

I would like to thank Nilüfer Bozbıyık, Sevinç Akdeniz and Onur Alkan for their valuable support on preparation of the volunteers for data collection.

I am eternally greatful to my family (Mr. Yıldırım Tuna, Mrs. Nesrin Tuna, and Mr. Necip Ali Tuna) for believing and supporting me all the time without hesitation.

I am especially grateful to my friends Murat Hepeyiler, Seda Şendur and Aslıhan Arslan who were always by my side during this thesis study and encouraged me when my motivation decreased and reminded me of the strength in me.

This thesis is a part of the project that is supported by The Scientific and Technological Research Council of Turkey (TUBITAK) via grant number 118C188 and entitled "New Generation Implant for All".

ABSTRACT

INVESTIGATION OF HIP JOINT KINEMATICS FOR DAILY LIFE ACTIVITIES

The daily life activities of a population have a significant effect on hip joint due to the repetitiveness and difficulty levels. Therefore, daily life activity data is an important source for manufacturing successive and long-lasting implants for hip joint arthroplasty. In this study, the hip joint kinematics is investigated under six determined activity that is performed frequently by the Turkish population. The collected and processed data is used in a TUBITAK funded project to form a first national database for the Turkish people.

The study first introduces the literature review on hip joint kinematics investigations for daily life activities. Thereafter, anatomy of the hip joint and motion capture techniques are explained.

Experimental procedure, protocol, materials, methodology and data collection are explained in detail in the Methodology Chapter. This Chapter introduces the determined daily life activities, chosen motion capture system and post-processing tools for the inverse kinematic analysis.

The Results and Discussion Chapter illustrates and tabulates the calculated results. Detailed explanations are made for discussing the results.

The Conclusion Chapter summarizes the study.

ÖZET

GÜNLÜK YAŞAM AKTİVİTELERİ İÇİN KALÇA EKLEM KİNEMATİĞİNİN İNCELENMESİ

Bir popülasyonun günlük yaşam aktiviteleri, gün içerisinde yapılma sıklığı ve zorluk derecesi nedeniyle kalça eklemi üzerinde önemli bir etkiye sahiptir. Bu nedenle, günlük yaşam aktivite verileri, kalça eklemi artroplastisi için başarılı ve uzun ömürlü implantların üretilmesi için önemli bir kaynaktır. Bu çalışmada kalça eklemi kinematiği, Türk popülasyonunda sıklıkla gerçekleştirilen altı belirlenmiş aktivite kapsamında incelenecektir. Toplanan ve işlenen veriler, Türk halkı için ilk ulusal veri tabanının oluşturulması amacıyla TÜBİTAK projesinde kullanılacaktır.

Çalışmada öncelikle günlük yaşam aktiviteleri için kalça eklemi kinematiği araştırmalarına ilişkin literatür taraması sunulmaktadır. Ardından kalça eklemi anatomisi ve hareket yakalama teknikleri anlatılacaktır.

Yöntem bölümünde deney protokolü, materyaller, metodoloji ve veri toplama ayrıntılı olarak anlatılacaktır. Bu bölümde, belirlenen günlük yaşam aktiviteleri, seçilen hareket yakalama sistemi ve ters kinematik analiz için veri işleme araçları tanıtılmaktadır.

Sonuçlar ve tartışma bölümü, hesaplanan sonuçları grafik ve tablo halinde verecektir. Sonuçların açıklaması tartışılma kısmında yapılacaktır.

Sonuç bölümü çalışmayı özetleyecektir.

ABBREVIATIONS

ADLs: Activities of Daily Life

CAST: Calibrated Anatomical System Technique

EMG: Electromyography

EMS: Electromagnetic Systems

IMUs: Inertial Measurement Units

ISB: International Society of Biomechanics

MOCAP: Motion Capture Systems

MRI: Magnetic Resonance Imaging

OMCs: Optical Motion Capture Systems

QTM: Qualisys Track Manager

ROM: Range of Motion

THA: Total Hip Arthroplasty

P.C.F: Participant Consent Forms

P.I.S: Participant Information Sheet

TABLE OF CONTENTS

LIST OF FIGURES

LIST OF FIGURES

Figure **Page**

LIST OF TABLES

CHAPTER 1

INTRODUCTION

Lower limb joints are the crucial points for the human movement during every task of human can perform. Human beings perform their daily life activities such as walking, lifting, bending, jumping by lower limb systems. The lower limb includes bones, joints, muscles, tendons to create a motion. Presence of any injury on the lower limb can affect the whole-body motion capability in a significant range according to the person's age or more over, general physical condition. Hip joint injuries are the most common and critical injuries over the populations. Since the hip joint transmits the whole-body weight to lower limb, it is a very important joint for human mobility. Any injury on the hip joint significantly reduces the range of motion capability of the joint. Hip joint arthroplasty (THA) is a practical and common solution for the fractured hip joint. The main aim of the THA is to replace the fractured joint with an implant to restore before-injury range of motion capability. However, the manufactured implants for THA are based on population data of the regions. That data is generally collected from gait activity that is performed by the volunteers. Additionally, daily life activities are also performed by the volunteers to obtain the movements that have a significant effect on the hip joints. Therefore, the collected data can be used for manufacturing more compatible implants for the target population. Since the collected data includes anthropometric data, it differs from nation by nation due to the physical differences. Therefore, manufactured implants cannot be suitable for every population on earth and can be expanded by including more daily life activities related with different cultures such as religious activities, meditational activities. Thus, a comprehensive investigation on hip joint can be conducted and more effective hip joint implants can be manufactured.

Hip joints are investigated by kinematic analysis to obtain range of motion capability of the joint. The kinematic analysis can be conducted by various methods. Motion capture methods are one of the most common techniques to investigate joint kinematics academically and clinically. The motion capture methods are separated into subtopics according to data collection and data processing types. The most common method is the opto-electronic motion capture system. The opto-electronics motion capture

systems are camera-based systems known as a gold standard. These systems use customized cameras, reflective materials or not using the reflective materials depending on the system, and a calibrated workspace. The non-opto-electronic motion capture systems are used in the literature widely. These motion capture systems use sensors to capture the movement and customized post-processing methods to process the data. The hip joint kinematics are investigated in literature by several motion capture methods to obtain range of motion for improving the prosthetics or developing new solutions.

The impact of the daily life activities on lower limb joints are investigated by several techniques in the literature. The literature survey is conducted on daily life activities and selected articles are tabulated in Table 1.

Table 1. Literature Survey on ADLs

Author	MOCAP System	Activities
Hyodo et al., (2017)	Electromagnetic (Fastrak)	22 ADLs including Putting on pants Putting on shoes Object picking
Charbonnier et al., (2015)	Magnetic Resonance Imaging (MRI) OMC (Vicon)	Stand to sit Lie down on the floor Lace the shoes (sitting) Object picking
Draicchio et al., (2010)	IMU OMC	Gait Seat-to-stand - stand-to-seat Squat Grasping Trunk flexion and rotation
Liang et al., (2020).	OMC (Qualisys)	12 ADLs including; Timed up and go Gait Obstacle crossing
Hemmerich et al., (2006)	Electromagnetic (Fastrak)	Squatting Kneeling Sitting cross-legged
Nakashima et al., (2014)	X-Ray Images	Gait Chair Rising Squatting Twisting
Sugano et al., (2012)	CT & OMC (Vicon)	Western style activities on the chair Japanese style activities on the ground

Hyodo et al. (2017) studied the lower limb joint kinematics by using 3-dimensional electromagnetic motion capture system (Fastrak, Polhemus, Colchester, VT) by performing 22 ADLs. The maximum - minimum angles and mean values of each joint

is calculated for each activity. The results showed that the maximum abduction-adduction and internal-external rotation of the hip joint occurs at maximum hip flexion while performing the putting on shoes. The performed ADLs also results that crouching and putting on pants cause greater joint angles. The obtained results are aimed to provide significant data for the THA operations.

Charbonnier et al. (2015) investigated the range of motion of the hip joint during daily life tasks under Magnetic Resonance Imaging (MRI), opto-electronic motion capture system (Vicon, Exford Metrics, UK) and physical examining to provide important data for hip prosthetics database. 4 healthy volunteers participated to the study. Motion capture data included 5 daily life activities due to their difficulties. The results showed that the abduction - adduction and internal - external rotation values stayed low and has a variety through the subjects.

Draicchio et al. (2010) studied the hip joint by using inertial measurement units. The joint angles are calculated in each plane of hip joint by performing gait, seat-to-stand & stand-to-seat, squat, grasping, trunk flexion and rotation. The study also compares inertial motion capture systems with opto-electronic motion capture systems to obtain accuracy.

Liang et al. (2020) studied on creating the first database of Asian-centric kinetic and kinematic data since there is no up-to-date Asian population database. The study is conducted by capturing the daily life activities the Asian people by using optical motion capture system Qualisys (Goteborg, Sweden) with force platform (Type 9260AA6, Kistler, Switzerland) on 10 healthy volunteers. 12 daily life activities that include gait, obstacle crossing is determined and investigated. The result of Liang et al. (2020) provides up-to-date lower and upper limb joint kinematics and kinetics data of Asian population to the aimed database.

Hemmerich et al. (2006) is also investigated the lower limb joints kinematics under high-range of motion activities during the daily life. Since western cultures effectively performs that has high-range motion activities, this study is specified 3 activity which are squatting, kneeling and sitting crossed-legged. These 3 activities are studied on 30 healthy volunteers by using electromagnetic motion capture system (Fastrak, Polhemus, Colchester, VT) and a force plate (BP400600NC, AMTI, Watertown, MA) to obtain kinematic and kinetics. The results showed that the hip angle reaches the maximum value in squatting.

Nakashima et al. (2014) studied the hip kinematics under the weight-bearing daily life activities. Hip joint kinematics is calculated by performing the activities of gait, chair rising, squatting and twisting. An X-Ray detector is used as a motion capture system to evaluate hip kinematics by a technique of model to image registration. Six healthy male volunteers are participated the experiments. The results showed that hip joint has a range over 100° in flexion and range over 60° in axial rotation.

Sugano et al. (2012) used a 4-dimensional motion capture system to study hip joint movement on deep bending activities after THA surgery. The selected activities are divided as Japanese style and Western style activities. The western style activities requires more range of motion than Japanese style activities in the hip joint. 55 Japanese female volunteers investigated in the study. According to the results, the highest range of motion is measured in picking up an object while sitting in the chair.

The aim of this thesis is to study daily life activities on hip joint kinematics and to provide results to a TUBITAK project. The data will be used for creating the first database of Turkish population.

The hip joint data is collected by an opto-electronic gold standard motion capture system. The data is processed, and a full body model will be built, thereafter the inverse kinematics analysis is performed to obtain joint angles of the hip. The study includes total of 22 healthy volunteers which performed 6 daily life activities.

1.1. Anatomy of the Hip Joint

Hip anatomy is the basic starting point to understand hip joint movements. Hip joint is a ball-and-socket joint that allows rotation in each axis. Figure 1 illustrates the hip joint's ball and socket structure. It provides balance during the stance and gait. Also, the whole upper body weight is transmitted through the hip joint. Thus, hip joint stability is highly crucial to maintain the motion and balance during daily life. Therefore, it effects the life quality as a core point.

Hip joint is composed of a ball, clinically known as femoral head, and a socket, clinically known as a pelvis or acetabulum. The surface of femoral head and acetabulum is covered by a biological material articular cartilage. The articular cartilage provides easier motion of the bones while protecting them.

Also, there is a space seen between femoral head and acetabulum in X-rays. That space is not complete void. Instead, a biological liquid named as synovial fluid is in between femoral head and acetabulum to provide smooth movement of hip joint. Absence of articular cartilage, synovial fluid or any damage on the femur or acetabulum affects the whole body, therefore effects quality of life. Figure 1. shows the hip joint structure.

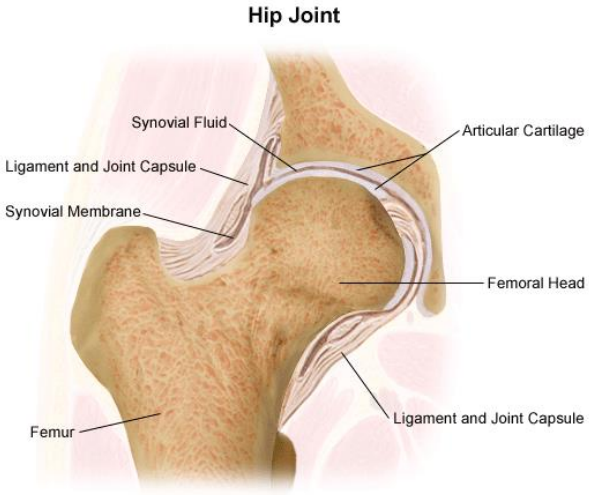

Figure 1. Hip Joint

The hip joint allows movements in three degrees of freedom which are flexion-extension, abduction-adduction, and internal-external rotation. These three rotations occur at three planes which are sagittal plane, frontal (coronal) plane and transverse plane. Figure 2 illustrates the hip joint rotations and planes which the rotations occur.

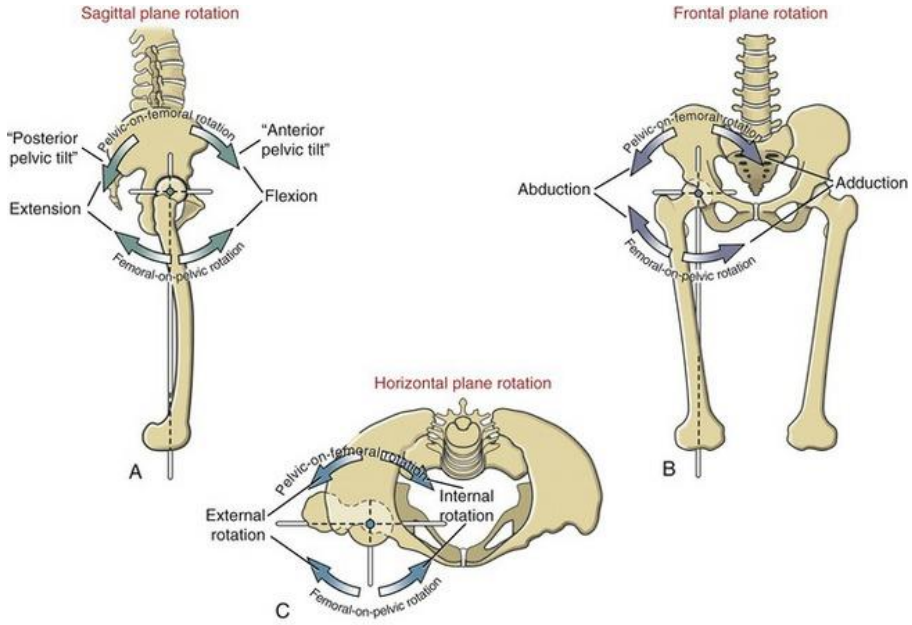

Figure 2. Planes of Hip Joint

- **Sagittal Plane Movement**

Sagittal plane movement has the largest plane motion of the hip joint. Flexion and extension occur on the sagittal plane and these movements are illustrated in Figure 3.

Flexion movement takes place on the swing phase of a gait cycle when the leg goes positive direction to become closer to the torso. Extension movement takes place on the stance phase of a gait cycle when the leg goes negative direction and moves away from the torso.

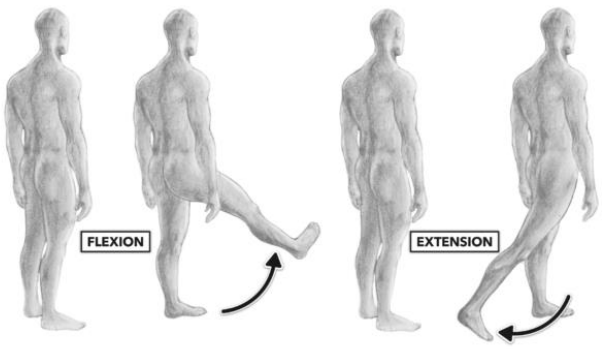

Figure 3. Flexion – Extension of Hip Joint in Sagittal Plane

- **Front (Coronal) Plane Movements**

Hip joint draws an arc during the abduction and adduction movement. During the abduction movement, the leg moves away from the body on the drawn arc. During the adduction movement, leg moves closer to the body. Abduction – adduction movement of the hip joint is illustrated in Figure 4.

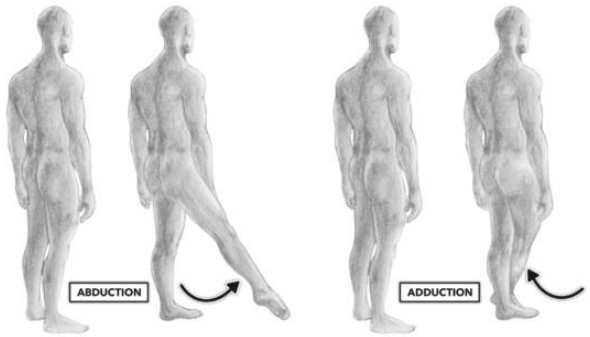

Figure 4. Abduction – Adduction of Hip Joint in Front Plane

- **Transverse Plane Movements**

Hip joint follows an arc during the external and internal rotation movements. During internal and external rotations, hip joint slightly rotates. Internal – external rotation movement of the hip joint is illustrated in Figure 5.

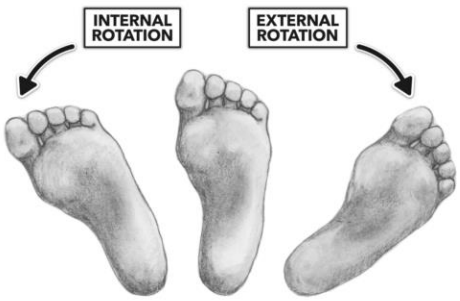

Figure 5. Internal – External Rotation of Hip Joint in Transverse Plane

1.2. Motion Capture Systems

The hip joint is monitored by a motion capture system in this thesis study. In the literature there are several motion capture systems that are available and are being used for clinical and academic applications. This section explains the motion capture systems in the literature.

Motion capture systems can be divided into two groups as Optical and Not-Optical Systems. Optical and Not-Optical systems are also divided into subgroups as seen in Table 2.

Table 2. Optical and Not-Optical Motion Capture Systems

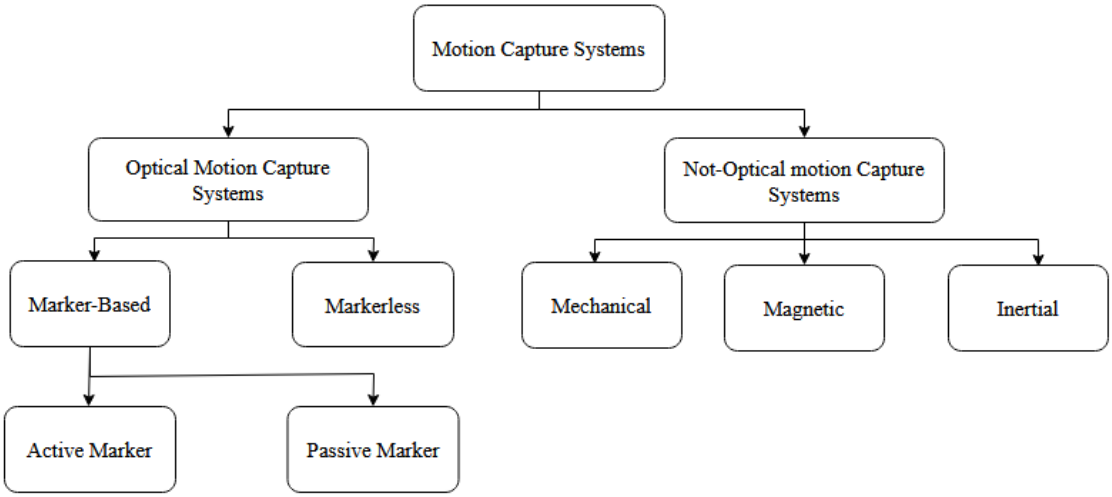

- **Optical Motion Capture Systems**

Optical or opto-electronic motion capture systems (OMCs) utilize customized infrared cameras to track the motion. The infrared cameras capture the motion of the object by make use of the markers which are placed at anatomical locations on the subject's body segments. OMCs utilizes the data captured by cameras, using the time-of-flight of light emitted from the markers to create 3-dimensional position and orientation for each marker. Thus, each segment's pose can be defined by their position and orientation.

OMCs are separated into two groups as with markers and without markers. OMCs with markers are separated into two groups by usage of marker types. OMCs with passive

markers make use of the markers which have a reflective surface, they reflect the light back to the cameras for the image to be formed. OMCs with active markers make use of the markers which have a source of light. They radiate infrared light to be captured by the cameras for the image to be formed.

Markerless OMCs uses artificial intelligence and image processing to track the movement. They are less accurate than marker-based OMCs.

OMCs are known as gold standards in literature due to their accuracy.

- **Non-Optical Motion Capture Systems**

Non-optical motion capture systems make use of sensors placed onto the segments of the subject. They are separated into three groups by data acquisition type.

  - **Inertial Motion Capture Systems**

Inertial motion capture systems consist of an accelerometer, a gyroscope, and a magnetometer.

The inertial measurement units (IMUs) measure angular rate, acceleration, and magnetic field vector in their local coordinate system. The IMUs are placed on a volunteer according to the positions defined for the suit to define body segments, positions, and orientations with respect to the reference coordinate system. Each IMU has 3 degrees-of-freedom accelerometer, 3 degrees-of-freedom magnetometer and 3 degrees-of-freedom gyroscope. Body segments, positions and orientations are defined according to the inertial measurement units by using gravitational acceleration, rotational velocity and orientation of the body. The IMUs collect the data and transfer it to the relevant software. Once the data is transferred to the computer environment, using a predefined model, motions can be visualized on the computer in real time. The inertial measurement units use quaternions, rotation matrices or Euler angles to define the segment's orientation. To define body segment orientations and positions, the acceleration readings obtained by the sensor are integrated by 2 times. The collected data can be transferred through wireless connection without hindering the natural motion flow of the subject (Figure 6).

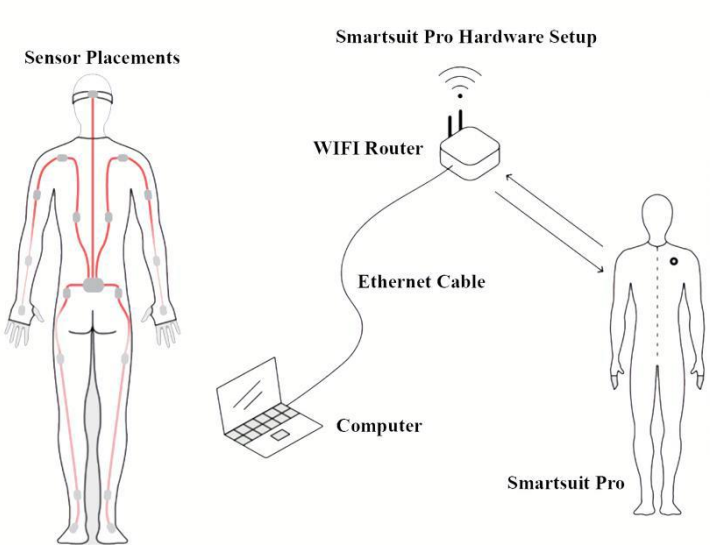

Figure 6. Inertial (IMU) Motion Capture System (Rokoko, Copenhagen, Denmark)

- **Electromagnetic Motion Capture Systems**

Electromagnetic systems (EMS) use electromagnetic sensors which emit magnetic waves that are connected to a computer to produce 3-dimensional data of the movement of the tracked object in real time. The movement is limited due to the connection of the sensors by cables (Figure 7).

(a) Transmitter (b) Receiver

Figure 7. Magnetic Motion Capture System (Polhemus, Vermont, Canada)

- **Electromechanical Motion Capture Systems**

Electromechanical motion capture systems also known as exoskeleton motion capture systems use sensors attached the body with a mechanical suit. The suit includes integrated mechanical sensors such as potentiometers to track the movement in real time without any processing of data (Figure 8)

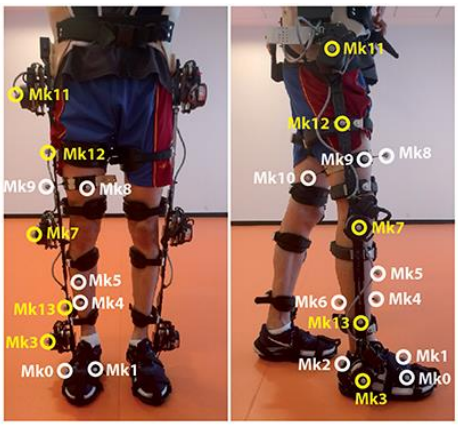

Figure 8. Exoskeleton MOCAP System

In this study, opto-electronic motion capture system is used for the data collection.

CHAPTER 2

METHODOLOGY

In this chapter, procedure, experimental protocol for the data collection, materials that are used in the experiment and methodology for performing the analysis is explained.

2.1. In Vitro Experiment

The in vitro study is conducted on measuring the marker reliability. Reliability of the marker data from the tracking cameras (Miqus M3) is measured by studying on an L-shaped wooden block which has a realistic anthropometric data of 5^{th} percentile Turkish female.

The in vitro study was conducted by constructing a setup which is designed as an L-shaped wooden block to mimic the profile of a human right leg. The dimensions of the L-shaped model are determined according to 5^{th} percentile Turkish female anthropometric data. The in vitro setup is driven by a servo motor, and the markers are placed on the setup as in Figure 9. There are IMU sensors in the Figure 9. The reason of that is the setup is also used in the TUBITAK project for measuring reliability between gold standard and a wearable motion capture system.

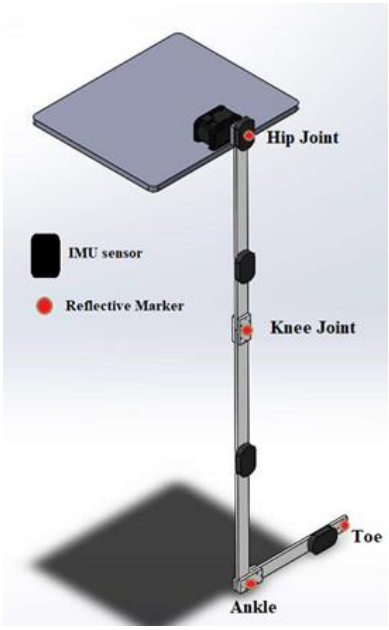

Figure 9. In Vitro Experimental Setup

Three constrained single plane motions flexion-extension, abduction-adduction and internal-external rotation of the hip joint are investigated.

Single plane motions of the hip joint are performed in a predetermined set of single plane fully constrained range of motion values by Dynamixel MX-64T servo motor. The predetermined range of motions are tabulated in Table 3 by referring to the anatomical sources related to the hip joint. The Dynamixel MX-64T servo motor was controlled by using an Arduino UNO board and supplied by TT TECHNIC QJ-3020S DC power supply.

Table 3. Range of Motion (RoM) of Hip Joint

Single Plane Motion	**Range of Motion (ROM)**
Flexion - Extension	130°/20°
Abduction - Adduction	40°/20°
Internal - External Rotation	30°/40°

The input is the controlled motion within a predetermined range of motion, and the output is the angle values at each frame. Each motion type was repeated 3 times for 3 sets of data recording sessions. The analysis is conducted to obtain range of motion, lower limit, and upper limit for each motion type.

In in vitro study, the Euler method and the Qualisys method are used to calculate the range of motion of the L-shaped model. The Euler method is implemented by writing a MATLAB code. According to the calculated results, RMSE value is calculated according to equation (1).

$$RMSE = \sqrt{\frac{\sum_i^n \left\| \|y_i - \hat{y}_i\| \right\|^2}{n}} \quad (1)$$

where n is the number of sample size, y_i is the I^{th} measurement and $\hat{y}_i$ is the prediction.

The results of mean, standard deviation and RMSE are given in Table 4.

The maximum RMSE is calculated as 0.8° for hip flexion. The RMSE values for hip joint movements are calculated as 0.80°/0.60° for flexion-extension, 0.67°/0.50° for abduction-adduction and 0.03°/0.13° for internal/external rotation. The reason for the high RMSE values could be explained by the experimental setup. There were minor position changes during the experiments due to action and reaction forces, which were caused by the start and stop motion of the motor unit.

Table 4. In Vitro Study Results of L-Shaped Model

Hip Joint Single Plane Motions with given inputs	**Qualisys (Mean ± Std)**	**RMSE**
Flexion (130°)	127.6° ± 0.04°	0.80
Extension (20°)	18.2° ± 0.01°	0.60
Abduction (40°)	38.0° ± 0.02°	0.67
Adduction (20°)	18.5° ± 0.01°	0.50
Internal Rotation (30°)	29.9° ± 0.20°	0.03
External Rotation (40°)	40.4° ± 0.05°	0.13

According to the obtained results, the standard deviation values of each movement for optical motion capture system (max std: 0.2° for internal-external rotation) are acceptable and indicates reasonable repeatability. Thus, it can be concluded that the marker tracking is reliable according to the results given in Table 4.

2.2. Procedure

In this section, the procedure of the study is explained by providing Ethics Committee Approval, consent and participation criteria.

2.2.1. Ethics Committee Approval and Consent

Data collection from human subjects requires an ethics permission. Therefore, receiving the ethics permission is a must before collecting data from healthy volunteers under the law. The ethics permission was obtained from the ethical committee of the Medical Faculty of İzmir Katip Çelebi University for the experiments.

After receiving the ethics permission approval, Participant Information Sheet (P.I.S) and Participant Consent Forms (P.C.F) were prepared to provide information to the volunteers. The P.I.S informs the participant about the procedure, the data collection,

the classified information, the exclusion criteria, the benefits, and the participant rights during the study. The P.C.F is obtained after the participant reads and understands the P.I.S. The Consent Form is vital for the experiment to start as it indicates participant will to conduct the *in vivo* study. The participants' questions are answered in detail in this stage of the study.

2.2.2. Participation Criterias

The participation criterias are determined to collect reliable data from the volunteers. Therefore, healthy volunteers are preferable for the study to constitute reliable database. Participation criterias for the study is determined under two subtopics as inclusion criteria and exclusion criteria. These criterias are tabulated in Table 5.

Table 5. Participation Criterias

Inclusion Criteria	**Exclusion Criteria**
• Participant must be 18 years old or older than 18 years old. • No suspicion or diagnosis of Covid-19 during the experiment. The HES code must be received.	• History of trauma in the lower body (hip, knee, foot, ankle). • Implants in the lower body (hip, knee, foot, ankle). • Pregnancy in female volunteers. • Allergies related to the materials to be used in the experiment. Body Mass Index (BMI) of 30 or above.

2.3. Selected Activities of Daily Life

The six daily life activities of Turkish population are selected to be performed in the experiments by the volunteers. The selected daily life activities are collected by using optical motion capture system Qualisys (Goteborg, Sweden). The six daily life activities are listed in Table 6. Protocol section explains the activities in detail.

Table 6. Determined Daily Life Activities

No.	Activity
1	Gait
2	Stoop Lifting
3	Squat Lifting
4	Asian Style Sitting
5	Ruku' to I'tidal
6	I'tidal to Sujud

2.4. Protocol

Each determined daily life movement is explained in detail in the Protocol section. In this section, it is explained how each selected movement affects the hip joint and how it will be performed by the volunteers. Experiments are carried out according to the determined protocol.

2.4.1. Gait

Walking is the primer reaction of travelling from a location to another for human beings by repetitive lower limb movement while preserving the stability. Therefore, every movement or activity includes natural transportation with body carried out by humans during their daily lives includes walking. Walking motion can have unique types for each human due to their physical health. Physical health includes the effects of internal effects such as age, lower limb conditions and external effects such as doing sports to improve body segments. However, the main reason that effects the walking pattern of a human is the lower limb joints which compose the motion. Any injury on the lower limb joints can cause a serious decrease in the person's walking quality. The hip injury is the most common type among the lower limb injuries that effect the walking, therefore the life quality of a person. Prostheses are the advanced solution for these highly critical injuries. Prostheses or implants are manufactured by collecting a certain population data to fit correctly. Walking is the motion that is investigated clinically to provide the data from the population. Clinically investigated walking motion is referred as "gait". The gait activity forms the backbone of the ISO 14242 standard which is used in the testing of hip

implants. Gait is a very complex motion that includes each lower limb joints. In this thesis, hip joint is the main focus.

Gait can be investigated through several motion capture methods. In this thesis, gait motion of volunteers is investigated with opto-electronic marker-based gold standard motion capture system.

The gait activity is analysed by examining the sagittal plane angles of lower extremities at heel strike and toe off moments of the event foot. The gait motion is composed of a cycle which begins and ends with heel strike or initial contact of same foot. Initial contact can be counted instead of heel strike due to walking characteristics. Each cycle is divided into two phases as stance phase and swing phase.

Stance phase is the complete period of the foot contacts with the ground, and it is illustrated in Figure 9. This phase begins with the initial contact of the foot and ends with when the foot loses its contact with the ground, in another name toe off.

Swing phase is the complete duration of the foot in the air. Swing begins with toe off and ends with initial contact.

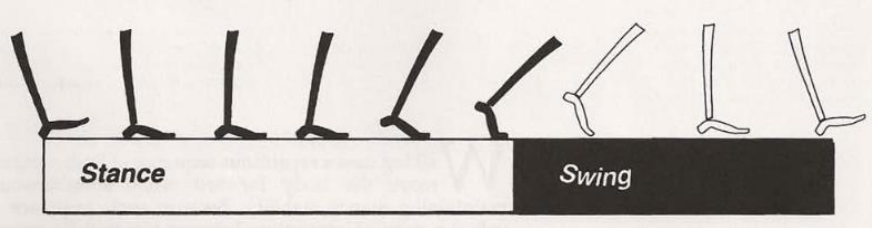

Figure 10. Stance and Swing Phases of Gait

Stance phase is also divided into three subphases as double stance, initial double stance or double limb support and single limb support. Stance phases of gait can be seen in Figure 10.

Double stance: This phase occurs where both foot is in contact with ground.

Initial double stance: This phase occurs where both feet are in contact with the ground. It occurs at the beginning of the cycle and after.

Single limb support: This phase begins with the opposite foot is lifted for swing.

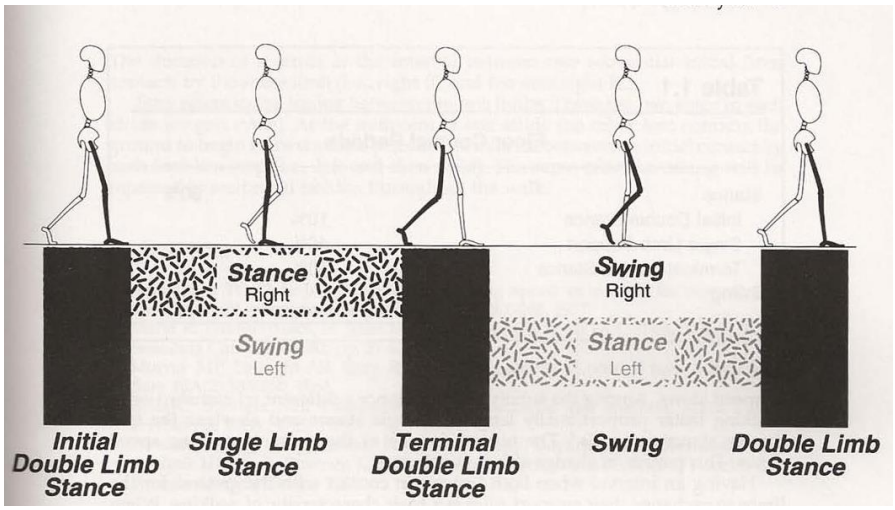

Figure 11. Stance Phases of Gait

The gait cycle can be identified by stride instead of stance and swing phases. One gait cycle is equal to one stride. The stride starts with initial contact of one foot and ends with initial contact of the same foot. The stride includes steps and there is total of 2 steps in a stride. Step and stride are illustrated in Figure 11. The steps can be defined also as the internal between two initial contacts.

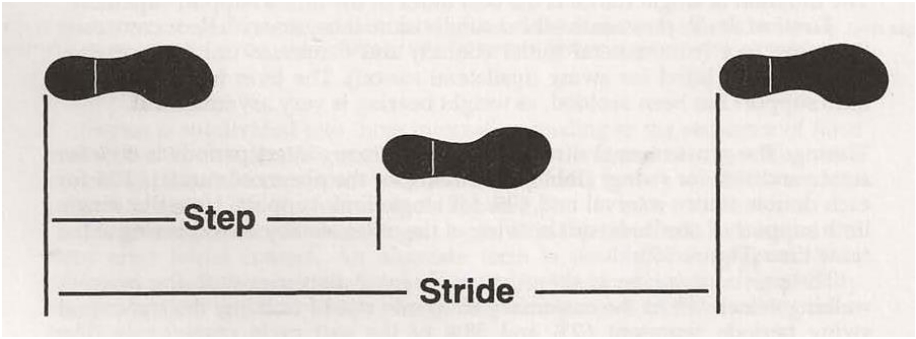

Figure 12. Step and Stride

The walking path for the gait activity is prepared to have 10m distance along the main axis of the laboratory with a 1m width. The volunteers are asked to perform gait motion as they do in their daily lives. Gait is shown in Figure 12 with its axis of motion.

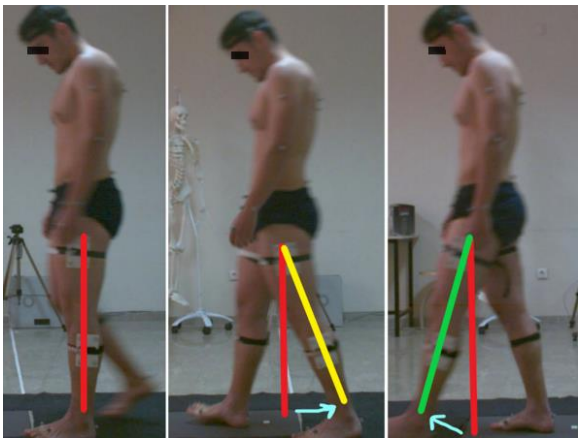

Figure 13. Axis of Motion in Gait of Hip Joint

2.4.2. Stoop Lifting

The volunteer is asked to be ready by standing still posture. When he/she is asked to start the activity, the following steps are followed:

The volunteer takes a step forward to the object that is positioned at a certain distance.

The volunteer bends towards the object from his/her hip without bending his/her knee to lift the object.

The volunteer drops the object back its original position.

The volunteer returns to upright posture without bending his/her knees (Figure 13).

During this activity, the trunk bends anteriorly and makes a flexion motion in the sagittal plane while the feet are stationary. The hip moves posteriorly and do an extension to maintain the balance of the body while leaning forward. Then, the body returns to the initial posture by doing the movements reversely to complete one cycle. For this motion, the body starts from the erect posture, and completes the lifting task to be back at an erect posture again.

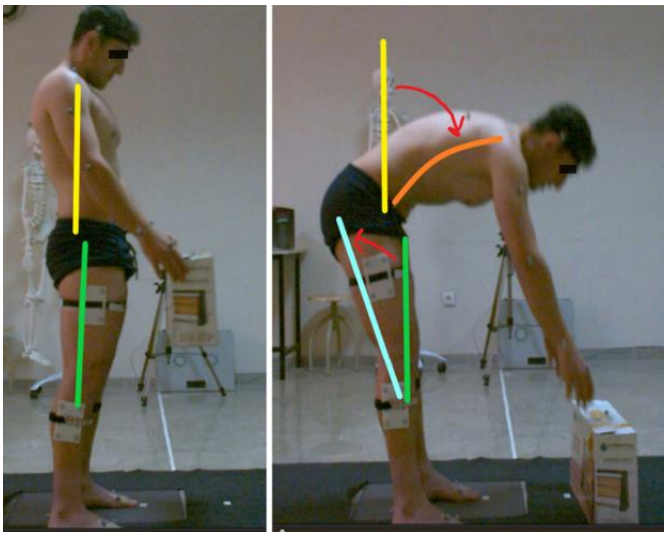

Figure 14. Stoop Lifting

2.4.3. Squat Lifting

The volunteer is asked to keep his/her the feet stationary on the ground while performing the activity. The following steps are followed:

The volunteer is asked to keep his/her feet stationary during the activity.

The volunteer performs a squat motion to lift the object which is positioned at a certain distance.

The volunteer drops the object its original position by performing squat motion again.

The volunteer returns his/her initial posture with squat motion. (Figure 14).

During this activity, a flexion moment occurs in the knee. Due to this moment, the hip moves posteriorly and extends to maintain the balance at the center of gravity.

The body also bends anteriorly and flexes. The body completes one cycle of the activity by starting from the erect posture and completing the lifting task at erect posture again.

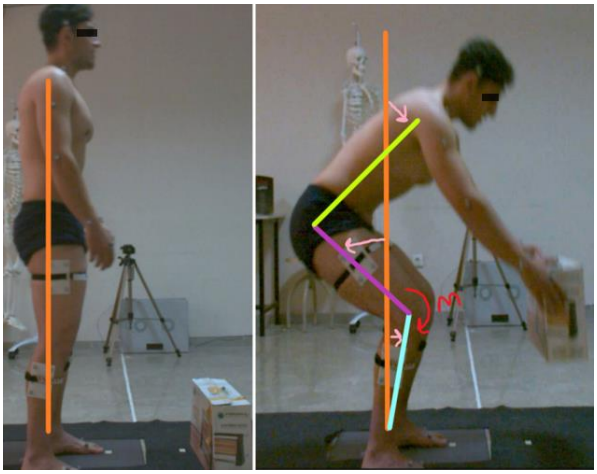

Figure 15. Squat Lifting

2.4.4. Asian Style Sitting

The volunteer is asked to be ready by standing still posture. When he/she is asked to start the activity, the following steps are followed:

The volunteer spreads his/her legs at shoulder level.

The volunteer bends his/her knees and moves forward to the ground till the hips are kept closer as possible to the ground.

The volunteer returns his/her initial posture by the reverse order to complete one cycle. (Figure 15).

In the Asian style sitting, plantarflexion occurs in the sagittal plane. The trunk performs flexion by creating flexion in the knees and hips. To maintain body balance, the arms also flex.

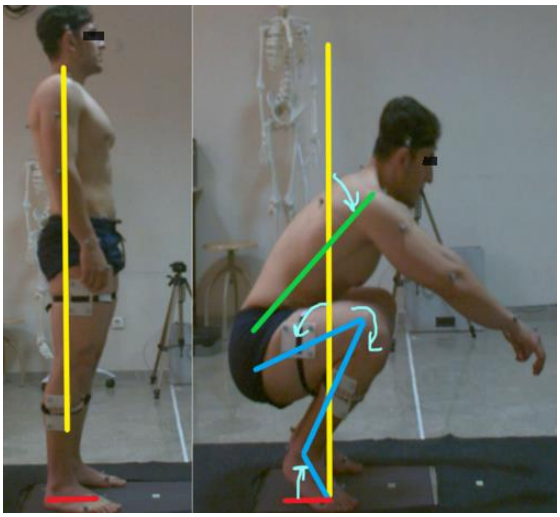

Figure 16. Asian Style Sitting

2.4.5. I’tidal to Ruku’

I’tidal to Ruku’ is an often movement performed by the majority of the Turkish people regarding to their religious believes. This activity consists of two parts. The first part is I’tidal and it is the upright position at the beginning. The second part is Ruku’ and it is the position where the volunteer’s hands are placed on the knees while leaning forward by bending the trunk. (Figure 16).

The volunteer is asked to be ready by standing still posture as I’tidal. When he/she is asked to start the activity, the following steps are followed:

The volunteer places his/her hands on the knees while the bending his/her trunk forward.

The volunteer returns the initial posture I’tidal.

The legs of the volunteer are kept fixed during the activity.

During this activity, the hip moves posteriorly and extend in the sagittal plane. The trunk, on the other hand, is flexed anteriorly. The volunteer completes one cycle starting from I’tidal and continue with Ruku’ and ends it with I’tidal position again.

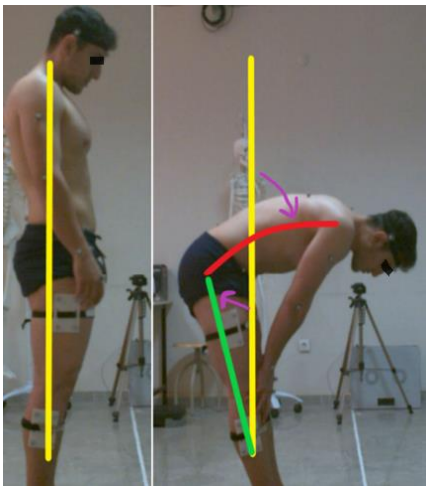

Figure 17. I’tidal to Ruku’

2.4.6. I’tidal to Sujud

Ruku to Sujud activity starts with I’tidal posture and ends with pre-prostration sit (Figure 17). This activity is particularly challenging to perform due the clusters at the thighs and shanks. Therefore, the volunteers are asked to perform the activity in a way that they feel comfortable during the motion.

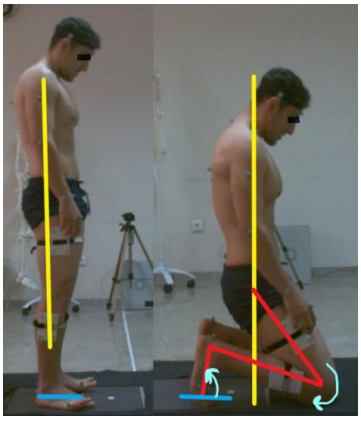

Figure 18. I’tidal to Sujud

2.5. Materials

In this section, the materials that are used in the study is explained in detail.

2.5.1. Qualisys Motion Capture System

The gold standard motion capture (MOCAP) system Qualisys (Goteborg, Sweden) is determined to be used for in vivo study. Qualisys Track Manager (QTM) is a tracking software which is designed for collecting precise and fast data from the model. The software captures 2D, 3D data in (X,Y) and (X,Y,Z) coordinates respectively, 6 degrees-of-freedom data in real time at a sampling rate of 100 Hz.

Qualisys motion capture system consists of 8 x Miqus3 Cameras (Figure 19), 1 x Miqus Video Camera, 50 Super Spherical Markers with Ø14 mm (Figure 19), Qualisys Track Manager 3D Software, Visual 3D Gait Analysis Software working on Research Module, DELSYS TRIGNO AVANTI 4 Channeled Wireless Surface EMG system (Delsys, Massachusetts, USA), and a BERTEC portable force platform (Quincy, USA). The Miqus M3 cameras have a resolution of 1824x1088 pixels in 2D and a resolution of 0.11 mm in 3D, in 10 cubic meters volume (Table 7). Qualisys make use of the markers which have a reflective surface, they reflect the light back to the cameras for the image to be formed. For this reason, it is very important the line of sight between the cameras and the markers are not blocked during the motion capture procedure. When the markers are not tracked by any of the cameras, the position of the marker cannot be detected. If the line continuity interrupted, the discontinuities are filled by an extrapolation method automatically embedded in the software. Although, extrapolated data is synthetic which sometimes may not represent the real motion. For this reason, a continuous line of sight is required for the markers to be detected by the system.

Figure 19. Miqus M3 Camera and Reflective Markers

Table 7. Qualisys (Goteborg, Sweden) Specifications

Normal Mode	2 MP (340 fps)
Hi-Speed Mode	0.5 MP (650 fps)
Resolution	1824x1088
3D Resolution	0.11 mm
Max. Capture Distance	15 m
Standard Lens	64x41°
Wide Lens	80x53°
Narrow Lens	44x27°
Sampling Rate	100 Hz
Software	Qualisys Track Manager
Marker Size	Ø14 mm
Calibration Wand Length	301.4 mm

Marker tracking requires a calibration process. The calibration of Qualisys system is a crucial step before performing the data collection because it defines the reference coordinate axis and the workspace which is highly important for markers to be fully tracked. Therefore, Qualisys system should be calibrated periodically to provide better results from marker tracking. The calibration is made by the calibration kit of the Qualisys system. The calibration kit includes a carbon fiber calibration wand with a precise length of 301.4 mm and an aluminum L-frame.

The marker tracker Miqus M3 cameras are distributed on the left and right walls of the laboratory in pairs of 3 at a 2m height from the ground, and 2 cameras are placed at the corner of the laboratory to provide better line-of-sight for marker tracking during the experiments. The video camera is placed on the right wall with a height of 1 meter from the ground and positioned to see the force platform which is located at the centre of the podium in the laboratory (Figure 20).

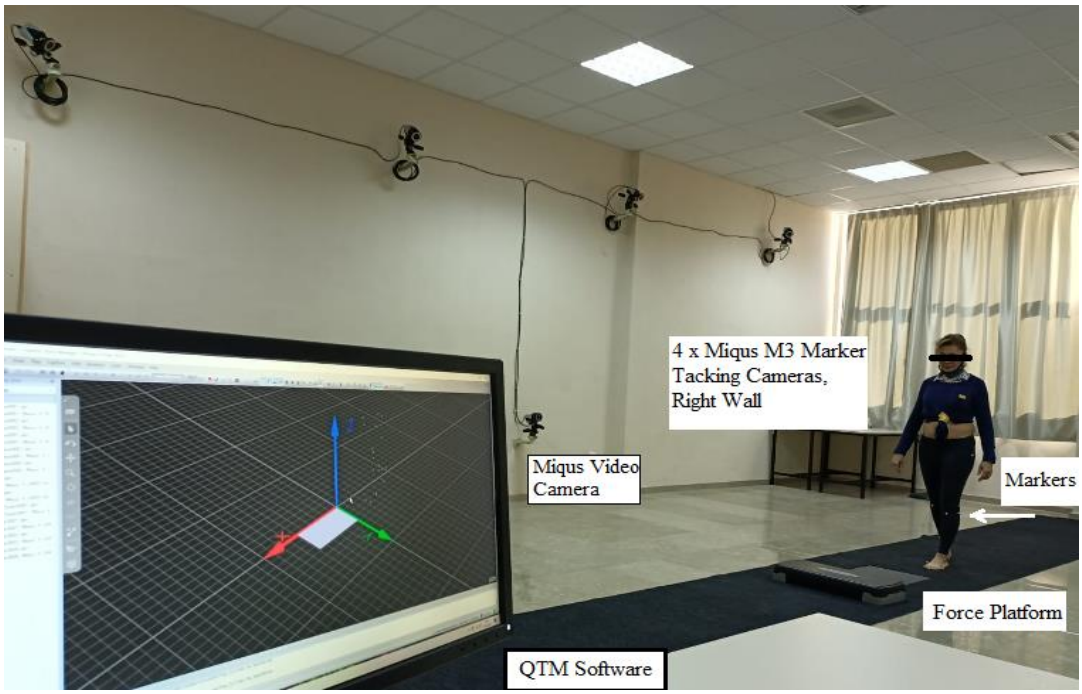

Figure 20. Biomechanics and Motion Capture Systems Laboratory

BERTEC portable force platform (Quincy, USA) is used to collect ground reaction force data from the volunteers to provide data for kinetics part of the project. The force platform has a dimension of 600 x 400 x 50 mm and positioned in the middle of the gait path. The force platform consists of 16 digital channels which measure forces and moments occur on each axis.

In this thesis, force data collected from force platform is not used and analysed. However, the data is used in the project for kinetics data collection apart from this thesis.

2.5.2. Visual3D Analysis Software

Visual3D is an analysis tool for biomechanical applications to measure tracked movement and collected force data by any 3-dimensional MOCAP system. Kinematics and kinetics analyses can be performed by using the tools within the software. Biomechanical models as body segments or skeletons, optimization methods, inverse kinematics calculations, signal processing methods and force structures to calculate kinetics can be utilized within the software by customized calculations.

Visual3D can be used for any activity collected from 3-dimensional motion capture systems to model, simulate and analysis. The main aim of using the Visual3D is to define body segments to create segments partially or full body skeleton model to conduct kinematics, kinetics calculations on defined segments.

In this thesis, Visual3D is used for the determined ADLs and Gait Activity to create the human skeleton model, simulation of the movements with the captured and processed data from Qualisys Track Manager and perform inverse kinematic analysis on the hip joint. The human model is created by the reference marker set which is used for defining the body segments.

2.6. Methodology and Data Collection

In this part of the thesis, the methodology and data collection process are explained in detail. The methodology part consists of the period of completion of the activities by the volunteer. The data collection process consists of data collection procedure from gold standard motion capture system and post-processing the collected data. Table 8. shows the flowchart of the methodology and data collection procedure beginning with preparation of volunteers.

Table 8. Methodology and Data Collection Diagram

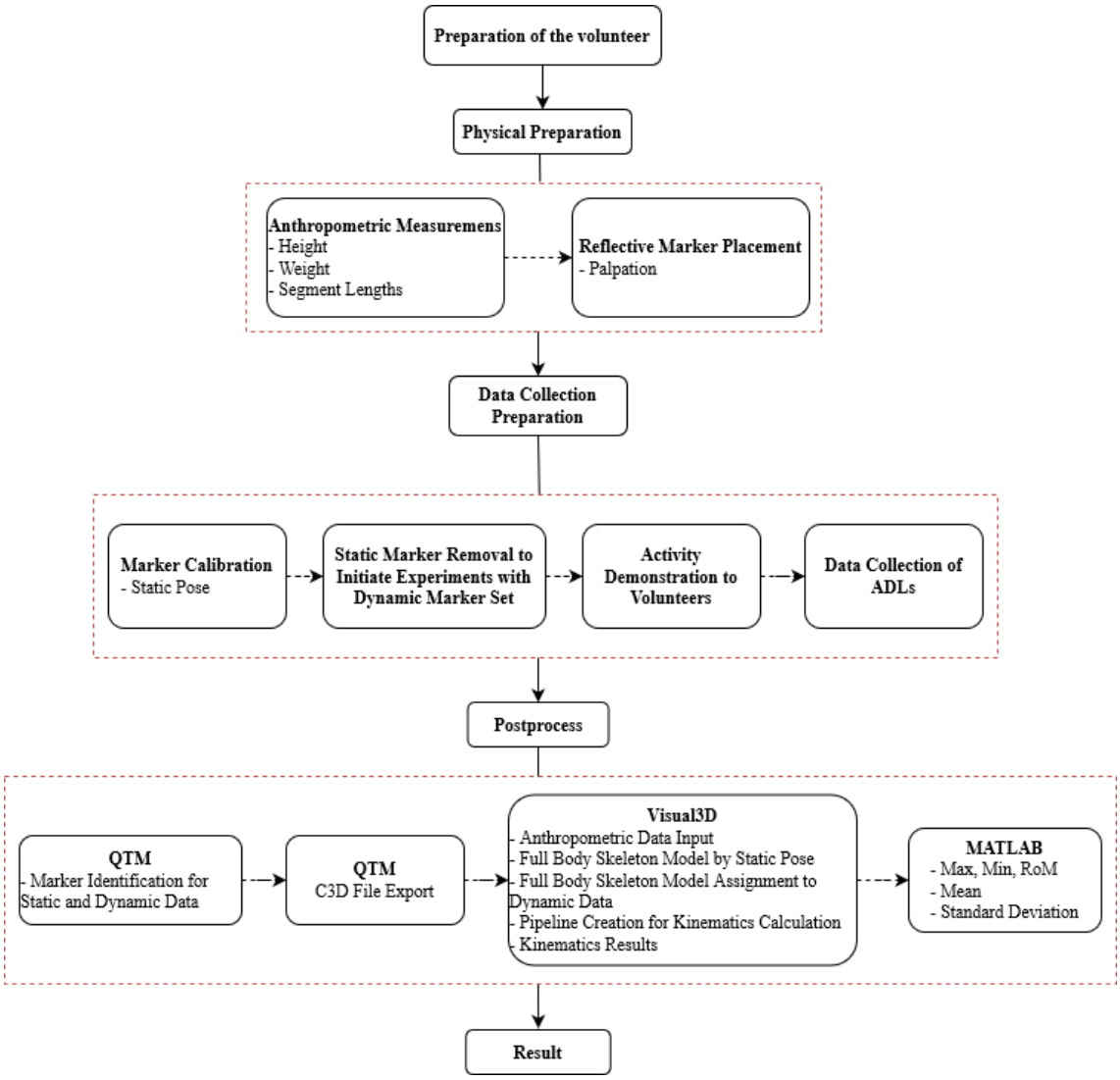

The gait and daily life activities are separated into two modules in Qualisys Track Manager for the experiment due to use of different modules.

Total of 22 volunteers participated to daily life activities (Age: 37.9 ± 10.81, Height: 1.73 ± 0.12 m, Weight: 72.35 ± 15.88 kg) and 21 (Age: 37.9 ± 10.87, Height: 1.73 ± 0.13 m, Weight: 73.05 ± 16.41 kg) volunteers participated to gait activity. The volunteers are participated from Mechanical Engineering Department of Izmir Institute of Technology.

The experiments are performed by the guidance of two qualified physiotherapists. The physiotherapists have taken the responsibility of measuring the body segments and locating the reflective markers on the correct anatomical locations of the body due to the

importance of the body segment measures and marker locations to build accurate segment models to avoid any user-based errors. However, since more than one physiotherapist has worked on the volunteers, there might be differences occurred while locating markers on the volunteer's body. Therefore, the results will be different if there is any significant difference between the two physiotherapists. Hence, the reliability between two physiotherapists is investigated by calculating the absolute mean differences of joint angles and the coefficient of determination (R^2) values to obtain if there is any significant difference occur in the results. The gait activity is selected for investigating the intra-tester reliability.

The intra-tester reliability tests are conducted on 3 volunteers by 2 physiotherapists. Results are investigated on hip, knee and angle joints at heel strike and toe off moments in sagittal plane by calculating mean angles and standard deviations. Then, the coefficient of determination (R^2) is calculated by conducting linear fitting method. The coefficient of determination (R^2) shows the agreement in a range from 0 to 1, where 0 shows the agreement failure and 1 shows the perfect fit for the agreement. The joint angles in sagittal plane results in smaller than 5° as it is reported minimal detectable changes in gait kinematics. The R^2 values are calculated 0.98 for hip joint, 0.96 for knee joint and 0.90 for ankle joint (Mihçin et al. 2023).

The first step before the volunteer performs the activities, the body segment, weight, and height measurements are taken. The body segments measurements include pelvis-medial, knee width, ankle width, sole delta, leg length, wrist width and thickness, elbow width, arm length, shoulder offset. In this stage, all measurements are taken from the same volunteers because the same data will be fed into another part of the project related with the kinetics.

Following the segment measurements, the volunteers are prepared for the data collection from the gold standard MOCAP system Qualisys.

The calibration process is completed with calibration kit. The T-shaped wand that has 2 markers at left and right ends of the stick is used for defining the workspace volume with L-frame which is placed at the centre of the laboratory to define laboratory axes. The workspace volume is constructed according to provide best line of sight for the cameras to observe the markers (Figure 21).

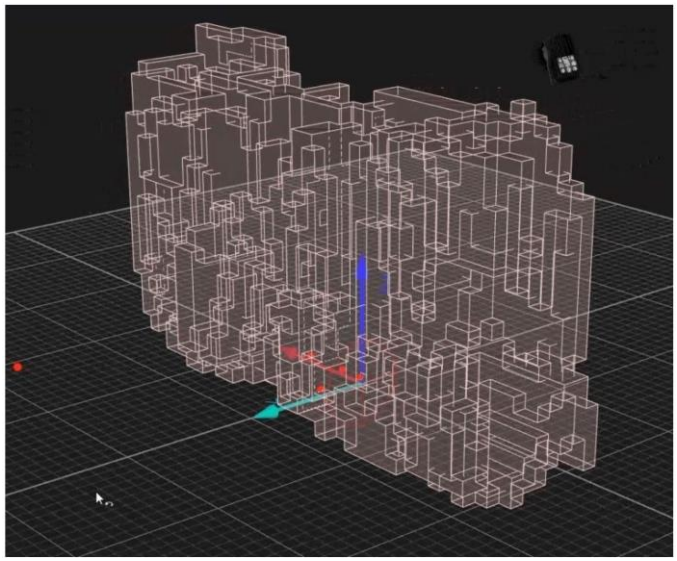

Figure 21. Calibrated Workspace Volume

Successful completion of the workspace leads to preparation of the volunteers for the data collection.

The reflective markers of the Qualisys system are placed onto the anatomical locations of the volunteer's body. That step requires careful placement of the reflective markers. The reason of that is, the retro-reflective markers of Qualisys MOCAP system are using for tracking human motion and conducting analyses by placing them onto the anatomical locations of the human body. Due to the physiotherapist's expertise, the anatomical landmarks are correctly found, and markers are placed. The markers are placed according to CAST Dynamic Full Body Marker Set and CAST Static Full Body Marker Set which are clinically proven marker sets defined by ISB (Figure 22). Although

there are several marker sets for the biomechanical studies, the CAST Full Body Marker Set is chosen specific to the ADLs and Gait to prevent line-of-sight problem.

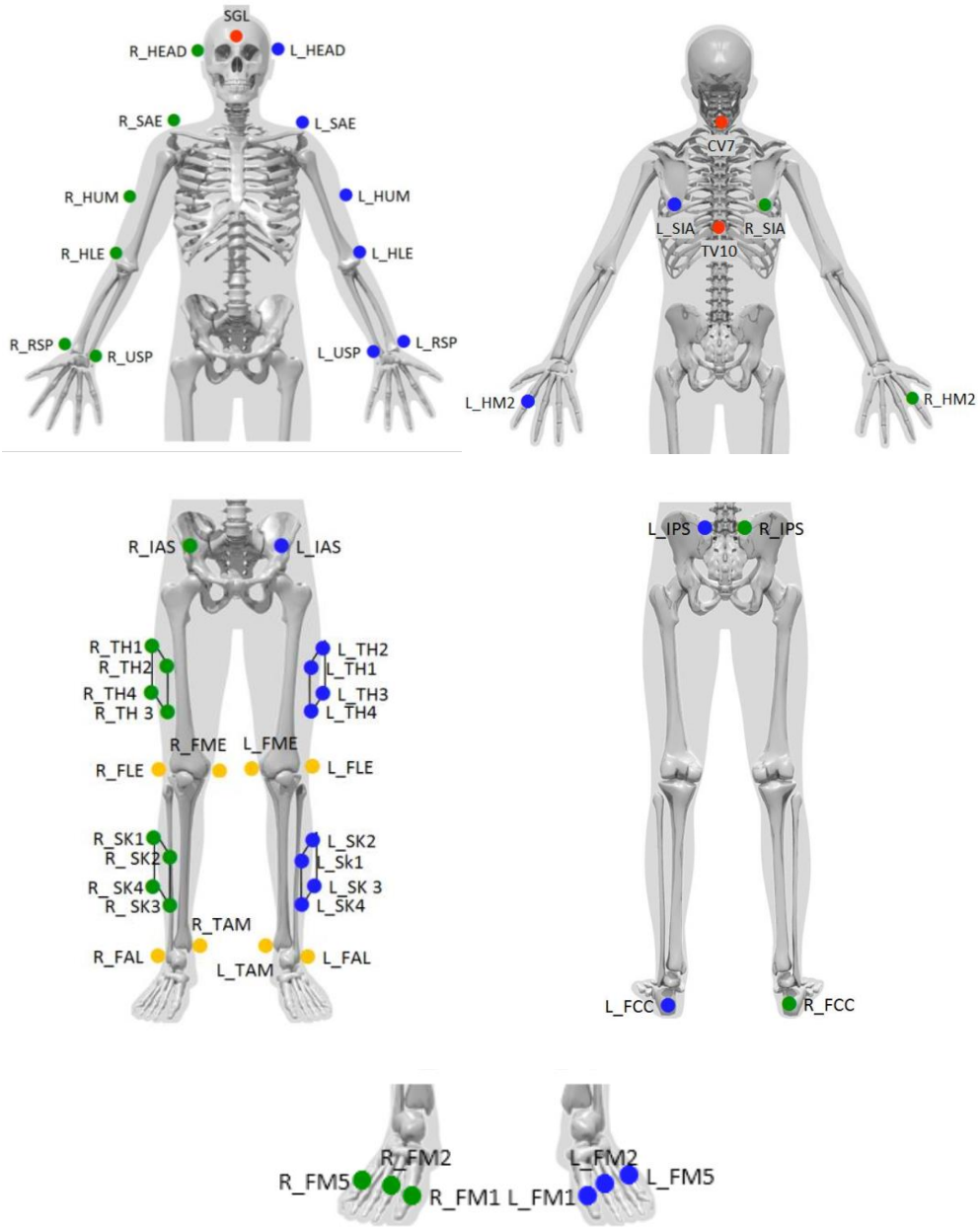

Figure 22. CAST Upper and Lower Body Marker Set

(Source: Cappozzo et al., 1995)

The anatomical landmarks of the body which markers are placed onto are defined in Figure 23 and 24.

Name	Ref. [1]	Location	Static (19)	Dyn. (19)
L_HEAD		Just above the ear	X	X
R_HEAD		Just above the ear	X	X
SGL	SGL	Glabulla	X	X
CV7	CV7	Cervical Vertebrae	X	X
L_SIA	SIA	Scapula - Inferior Angle	X	X
R_SIA	SIA	Scapula - Inferior Angle	X	X
TV10	TV10	Thoracic Vertebrae	X	X
L_SAE	SAE	Scapula - Acromial Edge	X	X
L_HUM			X	X
L_HLE	HLE	Humerus - Lateral Epicondyle	X	X
L_RSP	RSP	Radius - Styloid Process	X	X
L_USP	UPS	Ulna - Styloid Process	X	X
L_HM2	HM2	Basis of Forefinger	X	X
R_SAE	SAE	Scapula - Acromial Edge	X	X
R_HUM			X	X
R_HLE	HLE	Humerus - Lateral Epicondyle	X	X
R_RSP	RSP	Radius - Styloid Process	X	X
R_USP	USP	Ulna - Styloid Process	X	X
R_HM2	HM2	Basis of Forefinger	X	X

Figure 23. CAST Upper Body Marker Set List

(Source: Sint Jan et al., 2007)

Name	Ref. [2]	Location	Static (36)	Dyn. (28)
L_IAS	IAS	Anterior superior iliac spine	X	X
L_IPS	IPS	Posterior superior iliac spine	X	X
R_IPS	IPS	Posterior superior iliac spine	X	X
R_IAS	IAS	Right anterior superior iliac spine	X	X
L_TH1-4		Cluster	X	X
L_FLE	FLE	Lateral epicondyle	X	
L_FME	FME	Medial epicondyle	X	
L_SK1-4		Cluster	X	X
L_FAL	FAL	Lateral prominence of the lateral malleolus	X	
L_TAM	TAM	Medial prominence of the medial malleolus	X	
L_FCC	FCC	Aspect of the Achilles tendon insertion on the calcaneus	X	X
L_FM1	FM1	Dorsal margin of the first metatarsal head	X	X
L_FM2	FM2	Dorsal aspect of the second metatarsal head	X	X
L_FM5	FM5	Dorsal margin of the fifth metatarsal head	X	X
R_TH1-4		Cluster	X	X
R_FLE	FLE	Lateral epicondyle	X	
R_FME	FME	Medial epicondyle	X	
R_SK1-4		Cluster	X	X
R_FAL	FAL	Lateral prominence of the lateral malleolus	X	
R_TAM	TAM	Medial prominence of the medial malleolus	X	
R_FCC	FCC	Aspect of the Achilles tendon insertion on the calcaneus	X	X
R_FM1	FM1	Dorsal margin of the first metatarsal head	X	X
R_FM2	FM2	Dorsal aspect of the second metatarsal head	X	X
R_FM5	FM5	Dorsal margin of the fifth metatarsal head	X	X

Figure 24. CAST Lower Body Marker Set List

(Source: Sint Jan et al., 2007)

There is a difference between static and dynamic marker set in the lower body where the static marker set has 8 additional markers on the lateral and medial epicondyle (L_FLE, L_FME, R_FLE, R_FME) of the femur and lateral prominence of the lateral malleolus and medial prominence of the medial malleolus (L_FAL, L_TAM, R_FAL, R_TAM). These additional markers are named as static markers and they are used for building thigh, shank, and foot bones in static model of the body in Visual3D. The static markers are removed after static pose is recorded. Removal of the static markers does not cause any calculation problems or data distortion for the dynamic model since the leg segments of the model follow the tracking markers (R_TH1, R_TH2, R_TH3, R_TH4, R_SK1, R_SK2, R_SK3, RK4).

The participant's profile is created in the QTM separately for gait and daily activities and a session is initiated to record the movements. Figure 25 illustrates the static pose while the humerus and radius are at 90° and the palm is in the medial position. Two static poses are recorded as anterior and posterior for each subject. The number of the markers in the computer interface is counted, if the marker number is equal to 55 in these static poses, then the static poses are confirmed to be recorded as correct. Then, the experiment starts with gait activities. After the Gait, the volunteers start to perform the ADLs.

Figure 25. Anterior and Posterior Static Pose

2.7. Hip Joint Kinematics

Hip joint kinematics is calculated by assigning the collected marker positions onto a kinematic model. In order to have the kinematics results by means of joint angles, inverse kinematics analysis is conducted on the selected kinematic model. The knee and ankle joints are included to the kinematic model in order to calculate range of motion of the hip joint. The kinematic model is a lower body model which is an open kinematic chain. Figure 26. shows International Society of Biomechanics (ISB) recommendation of kinematic hip model.

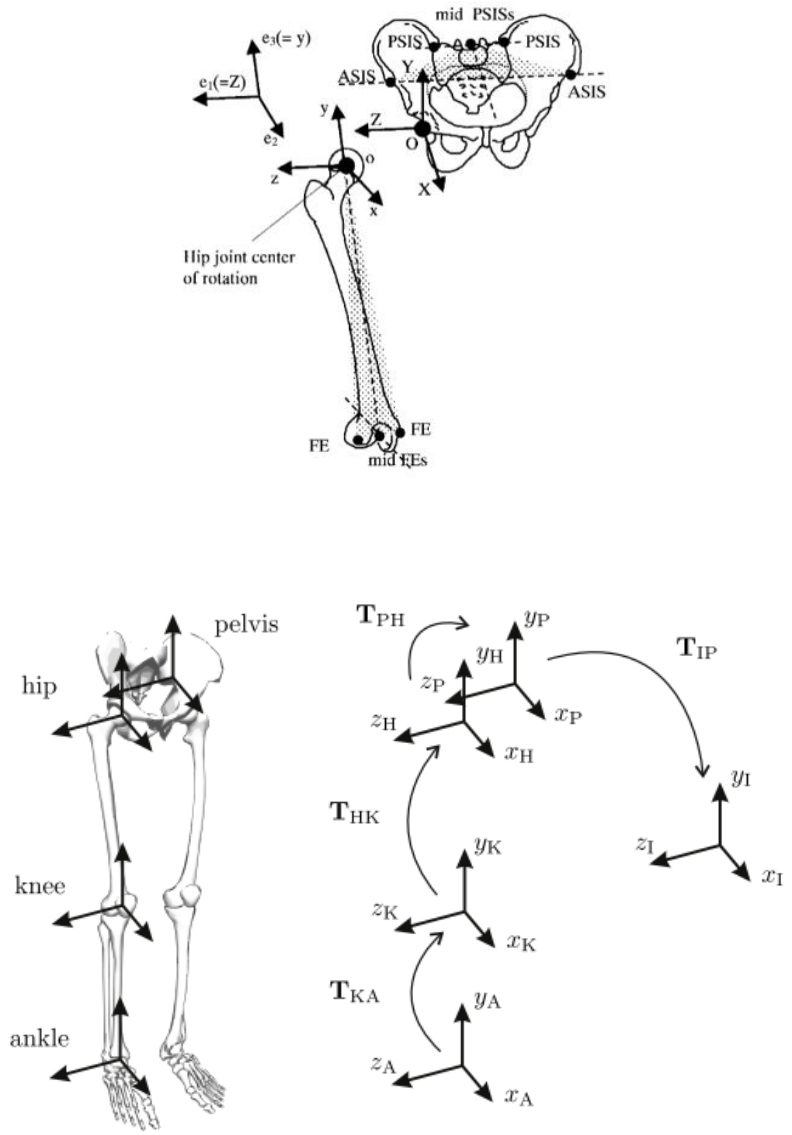

Figure 26. Hip Joint Anatomical Coordinate Reference by ISB

According to the recommended model from ISB, each segment has its reference frame at the joint centre which connects one segment to the other. Hence, the inertial frames and frames of the segments are aligned. Therefore, x axis points forward (anteriorly), y axis points upwards (superiorly) and z axis points to the right side.

According to the model in Figure 26, the homogeneous transformation matrices can be written for pelvis, hip, knee, and ankle as in equation (2).

$$\mathbf{T_{IP}} = \begin{bmatrix} \mathbf{R}_{\mathrm{IP}} & \mathbf{r}_P^I \\ \mathbf{0}_{1x3} & 1 \end{bmatrix} \quad \mathbf{T_{PH}} = \begin{bmatrix} \mathbf{R}_{\mathrm{PH}} & \mathbf{r}_H^P \\ \mathbf{0}_{1x3} & 1 \end{bmatrix}$$
$$\mathbf{T_{HK}} = \begin{bmatrix} \mathbf{R}_{\mathrm{HK}} & \mathbf{r}_K^H \\ \mathbf{0}_{1x3} & 1 \end{bmatrix} \quad \mathbf{T_{KA}} = \begin{bmatrix} \mathbf{R}_{\mathrm{KA}} & \mathbf{r}_A^K \\ \mathbf{0}_{1x3} & 1 \end{bmatrix} \tag{2}$$

where $\mathbf{R}_{\mathrm{IP}}$, $\mathbf{R}_{\mathrm{PH}}$, $\mathbf{R}_{\mathrm{HK}}$, $\mathbf{R}_{\mathrm{KA}}$ are rotation matrices; $\mathbf{r}_P^I$, $\mathbf{r}_H^P$, $\mathbf{r}_K^H$, $\mathbf{r}_A^K$ are the position matrices.

$\mathbf{R}_{\mathrm{IP}}$: Orientation of the pelvis frame relative to inertial frame.

$\mathbf{r}_P^I$: Position of the pelvis frame relative to inertial frame.

Pelvis markers can be represented in inertial frame, as in the equation (3)

$$\mathbf{m}_{P,j}^I = \mathbf{r}_P^I + \mathbf{R}_{\mathrm{IP}}\mathbf{p}_{P,j}^P \tag{3}$$

where $\mathbf{m}_{P,j}^I$ is the pelvis marker measured in inertial frame. Therefore, it can be written as homogeneous coordinates as in equation (4), where j is the j^{th} of pelvis marker.

$$\begin{bmatrix} \mathbf{m}_{P,j}^I \\ 1 \end{bmatrix} = \mathbf{T_{IP}} \begin{bmatrix} \mathbf{p}_{P,j}^P \\ 1 \end{bmatrix} \tag{4}$$

Then, the transformation matrix for the hip joint can be found as in equation (5)

$$\begin{bmatrix} \mathbf{m}_{T,j}^I \\ 1 \end{bmatrix} = \mathbf{T_{IP}} \begin{bmatrix} \mathbf{p}_{T,j}^H \\ 1 \end{bmatrix}, \quad j = 1, \ldots, M_T$$

$$\mathbf{T_{IH}} = \mathbf{T_{IP}}\mathbf{T_{PH}} \tag{5}$$

where M_T is the thigh marker in thigh frame and j indicated the j^{th} of M_T marker.

Qualisys Track Manager has several techniques to calculate orientation of segments. The main technique that the QTM uses is the Euler angle method. Euler angle

calculation uses rotation matrices to obtain a 6 degrees-of-freedom rigid body pose. The rotation matrices are defined as R_x, R_y and R_z as rotation about X, Y and Z axes with the angles of roll (θ), pitch (φ) and yaw (ψ). The roll (θ), pitch (φ) and yaw (ψ) rotations can be seen in Figure 27 to clarify the rotation axes according to a global reference frame.

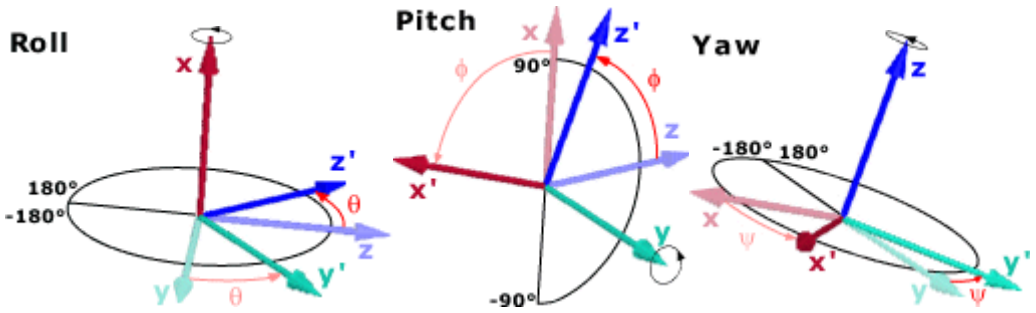

Figure 27. Roll, Pitch and Yaw Axes

As seen in Figure 27, the roll angle occurs about X axis, the pitch angle occurs about Y-axis and yaw angle occurs about Z axis. The ranges of the rotation angles are given also in the Figure 27. The rotation angles can define any orientation of a rigid body in the related range of motions.

The rotation matrix R is calculated by multiplying each rotation matrix in a determined order. The reason for that is, if the order of the multiplication is changed, then the resulting rotation matrix R would be changed. Therefore, the order should be determined before conducting the calculations. The rotation matrices for each axis of rotation are given in equation (6) and the rotation matrix of the XYZ Euler sequence is given in equation (7) and (8).

$$R_x = \begin{bmatrix} 1 & 0 & 0 \\ 0 & cos\theta & -sin\theta \\ 0 & sin\theta & cos\theta \end{bmatrix} \quad R_y = \begin{bmatrix} cos\Phi & 0 & sin\Phi \\ 0 & 1 & 0 \\ -sin\Phi & 0 & cos\Phi \end{bmatrix}$$

$$R_z = \begin{bmatrix} cos\Psi & -sin\Psi & 0 \\ sin\Psi & cos\Psi & 0 \\ 0 & 0 & 1 \end{bmatrix} \tag{6}$$

$$\mathbf{R} = \mathbf{R_x}.\mathbf{R_y}.\mathbf{R_z} = \begin{bmatrix} r_{11} & r_{12} & r_{13} \\ r_{21} & r_{22} & r_{23} \\ r_{31} & r_{32} & r_{33} \end{bmatrix} \quad (7)$$

$$\mathbf{R} = \begin{bmatrix} cos\Phi cos\Psi & -cos\Phi sin\Psi & sin\Phi \\ cos\theta sin\Psi + cos\Psi sin\theta sin\Phi & cos\theta cos\Psi - sin\theta sin\Phi sin\Psi & -cos\Phi sin\theta \\ sin\theta sin\Psi - cos\theta cos\Psi sin\Phi & cos\Psi sin\theta + cos\theta sin\Phi sin\Psi & cos\theta cos\Phi \end{bmatrix} \quad (8)$$

The rotation angles can be found by using equation (9)

$$\Phi = \arcsin(r_{13}) \qquad \theta = \arccos(\frac{r_{33}}{cos\Phi}) \qquad \Psi = \arccos(\frac{r_{11}}{cos\Phi}) \quad (9)$$

The second technique that is used for calculating angle or range of motion of a rigid body is a vector-based method. At least 3 markers are used to calculate the angle between 2 vectors. To calculate the angle between two lines, the QTM demands to identify the markers that will be used in the calculation. Thus, the calculation can be performed according to equation (10).

$$OA = (x_a - x_0,\ y_a - y_0, z_a - z_0)$$
$$OB = (x_b - x_0,\ y_b - y_0,\ z_b - z_0)$$

$$AB = |OA||OB|cos\alpha \qquad \text{and} \qquad A \times B = ABsin\alpha,$$

$$tan\alpha = \frac{A \times B}{AB} \quad (10)$$

The output of the calculation can be received as TSV or MATLAB data format to investigate.

2.8. Postprocessing of the Data

Postprocessing of the collected data starts with labelling the reflective markers properly in QTM. It is a very crucial step for the analysis because mislabeled markers

can affect the results. Therefore, the markers are labelled according to chosen CAST Marker Set. Firstly, the static pose is labelled. Then, dynamic labelling is performed on collected ADLs and Gait. There is another crucial step is to identify all markers. If there is a line-of-sight issue according to the performed activity, the missing marker period must be filled with correct extrapolation method. Extrapolation methods in QTM are static, linear, polynomial, relational, virtual, and kinematic. The most used methods in this thesis are linear, polynomial, relational and virtual. Relational extrapolation method is used for filling the gap between two frames by using a marker to define origin, a marker to define x direction and a marker to define xy-plane for the missing marker. Relational extrapolation method is used similarly for filling the gap between two frames for the missing marker. The difference between relational and virtual extrapolation methods is that virtual method is used for a marker that encounters line-of-sight problem and not visible during the activity cycle.

The cycle is selected after the labelling operation. The cycle of each activity is described in Section 2.4. Accordingly, the determined cycle is exported as a C3D file to be used in Visual3D. The C3D file contains 3-dimensional coordinate and numeric data from performed activities. The C3D file includes all different parameters, e.g. anthropometric measures, describing the data in one single file.

Visual3D uses the exported C3D files from QTM to model the body segments or skeletal models. The C3D file of each activity and the static pose are imported to the software. In order to conduct inverse kinematics analysis on hip joint, a pipeline is written. The pipeline is a tool that can be customized by choosing the steps and calculations to perform the modelling and analysis sections. In the pipeline, the following steps are followed:

Static pose file is chosen to assign the segments according to the defined locations. (Figure 28)

The full body skeleton template is chosen to build the model.

All activity files that will be analysed are chosen.

The weight and height of the volunteer is fed into the analysis.

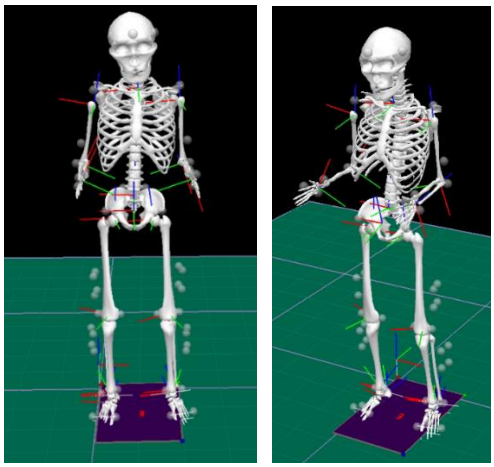

Figure 28. Static Full Body Model in Visual3D

The files are red and analysed by using inverse kinematic method with defined order for hip joint.

The results are exported for each activity to their own directories after completing the inverse kinematic analysis. The results contain the full range of motion data of a cycle for each activity. However, the exported results are separated and do not give clear information about total range of motion, mean, standard deviation and upper-lower limits of the total collected data. Therefore, a MATLAB code is prepared to calculate these measurements and to acquire population plots by means of each axis of hip joint.

CHAPTER 3

RESULTS AND DISCUSSION

In this chapter, the results of the performed activities are given, and discussions are made according to the results.

3.1. Results of Gait and ADLs

The ADLs and Gait activity data collected from the gold standard motion capture system were processed and analyzed by using Qualisys Track Manager, Visual3D and a code is written with MATLAB.

Inverse kinematic analysis was performed by Visual3D via C3D files which contain all information about the collected data from the volunteers.

Thereafter, the maximum and minimum joint angles were identified to calculate range of motion (ROM) values of each axis of hip joint for each set of activity.

Since the aim is to define the range of motion variability of hip joint among a determined population, statistical methods were utilized. The mean and standard deviation calculations of each set of activity were made to obtain the amount of variability of calculated range of motion for each activity. Standard deviation gives the variability of data from its mean value. Low values of standard deviation indicate good accuracy and repeatability of the measurements.

The variance through the volunteers on same activities can be obtained by adding and subtracting the calculated standard deviation value from the mean of the data. Thus, the upper and lower limits of the range of motion data can be calculated for each set of activity. Although, the range and values differed from each other for each volunteer, a similar pattern in the curves is observed for each activity.

Mean of all the collected data for each motion and each joint is calculated by

$$\bar{x} = \frac{\sum_{i=1}^{n} x}{n} \tag{11}$$

where, x is each value of sample, n is the number of sample size and $\bar{x}$ is the mean value of the sample.

The standard deviation is calculated by

$$\sigma = \sum_i^n \sqrt{\frac{(x_i - \bar{x})^2}{n}} \tag{12}$$

where σ is the standard deviation, x_i is the i^{th} value of the sample and $\bar{x}$ is the mean.

The range of motion (ROM) of a joint movement can be calculated by subtracting the maximum and the minimum value of the sample from each other to calculate the absolute value.

$$ROM = |x_{max} - x_{min}| \tag{13}$$

The results are plotted and tabulated for each set of activity. The legend of the graphs refers to mean, upper and lower boundaries of the range of motion (Figure 29). Fill command is used for coloring the range of motion variation between upper and lower boundaries.

Figure 29. Legends of Result Plots

The figures show the angular range of motion for each set of activity within cycle percentage. Each activity has 100% percentage range for a cycle. Since each activity can be performed with different durations for each volunteer, a normalization process was conducted on the data to obtain range of motion variability in same percentages. Thus, the subjectivity in the analysis was eliminated. The normalization process was performed by converting the time values into cycle percentages to eliminate the time dependency by interpolating the selected sample time as a reference in the process.

3.2.1. Gait

Gait activity is performed by 21 volunteers. The maximum, minimum and range of motion values of each hip joint axis are found and tabulated in Table 9.

The hip joint has a flexion-extension range of motion of 34.28° with maximum angle of 25.99° and minimum angle of -8.29°. The hip joint has an abduction-adduction range of motion of 1.15° with maximum angle of 0.99° and minimum angle of -2.15°. The hip joint has an internal-external rotation range of motion of 1.76° with maximum angle of 0.31° and minimum angle of -1.45°.

Table 9. Max., min., and RoM Values of Hip Joint in Gait

	Gait		
	Max	Min	RoM
Hip F-E	25.99°	-8.29°	34.28°
Hip ABD-ADD	0.99°	-2.15°	1.15°
Hip I-E ROT	0.31°	-1.45°	1.76°

Dynamic models that were created in Visual3D for Gait are given in Figure 30.

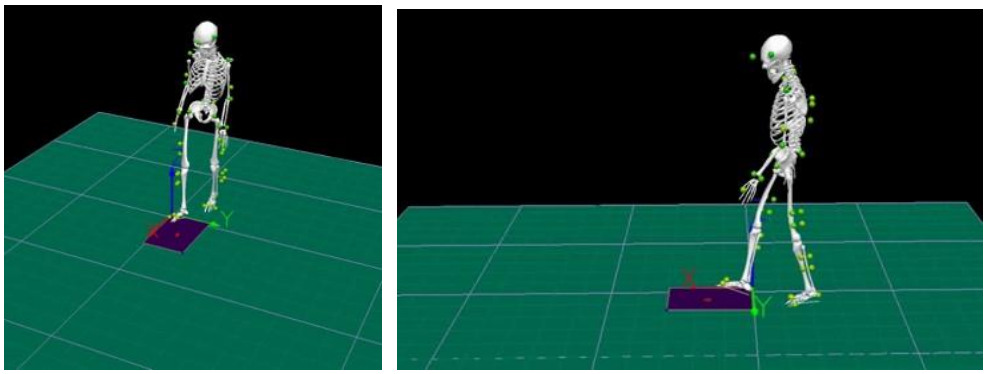

Figure 30. Dynamic Full Body Model of Gait in Visual3D

Figure 31 shows the variability of the motion through volunteers by taking account mean and standard deviation.

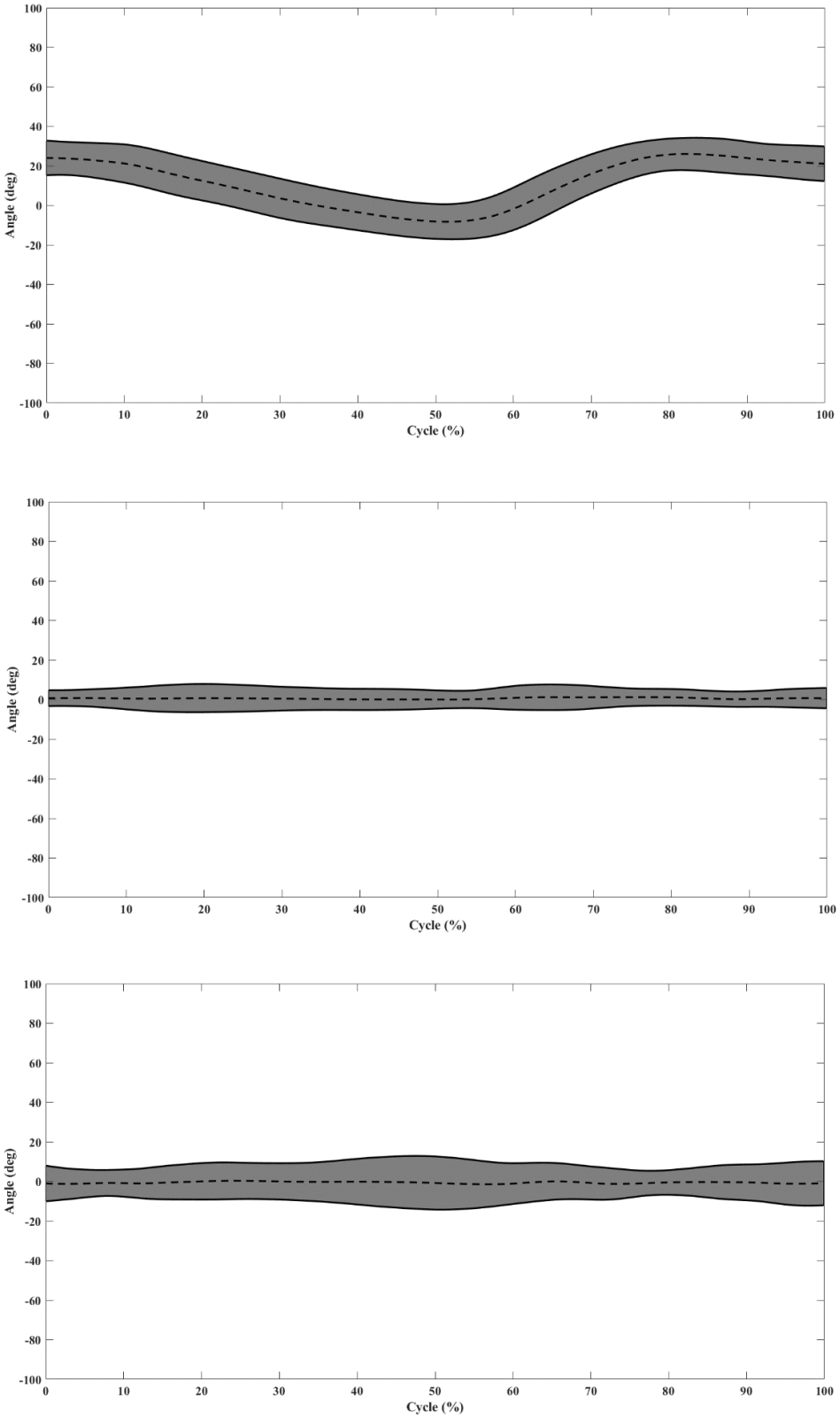

Figure 31. Hip Joint Range of Motion for Gait

As stated before, the range of motion plots show the behavior and limits of joint movements for each motion. The hip flexion-extension and internal-external rotation

movement have considerably higher standard deviation value compared with abduction-adduction movement of the hip joint. Since step length, leg length and other dependencies can affect a person's walk style, this variance could be expected.

3.2.2. Stoop Lifting

The maximum, minimum and range of motion values of each hip joint axis are found for Stoop Lifting activity and tabulated in Table 10.

The hip joint has a flexion-extension range of motion of 64.17° with maximum angle of 64.73° and minimum angle of 0.56°. The hip joint has an abduction-adduction range of motion of 1.41° with maximum angle of 1.72° and minimum angle of 0.31°. The hip joint has an internal-external rotation range of motion of 4.58° with maximum angle of 3.12° and minimum angle of -1.46°.

Table 10. Max., min., and RoM Values of Hip Joint in Stoop Lifting

	Stoop Lifting		
	Max	Min	RoM
Hip F-E	64.73°	0.56°	64.17°
Hip ABD-ADD	1.72°	0.31°	1.41°
Hip I-E ROT	3.12°	-1.46°	4.58°

Dynamic models that were created in Visual3D for Stoop Lifting are given in Figure 32.

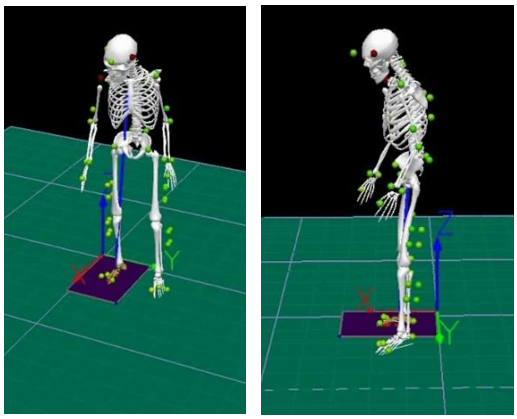

Figure 32. Dynamic Full Body Model of Stoop Lifting in Visual3D

Figure 33 shows the variability of the motion through volunteers by taking account mean and standard deviation.

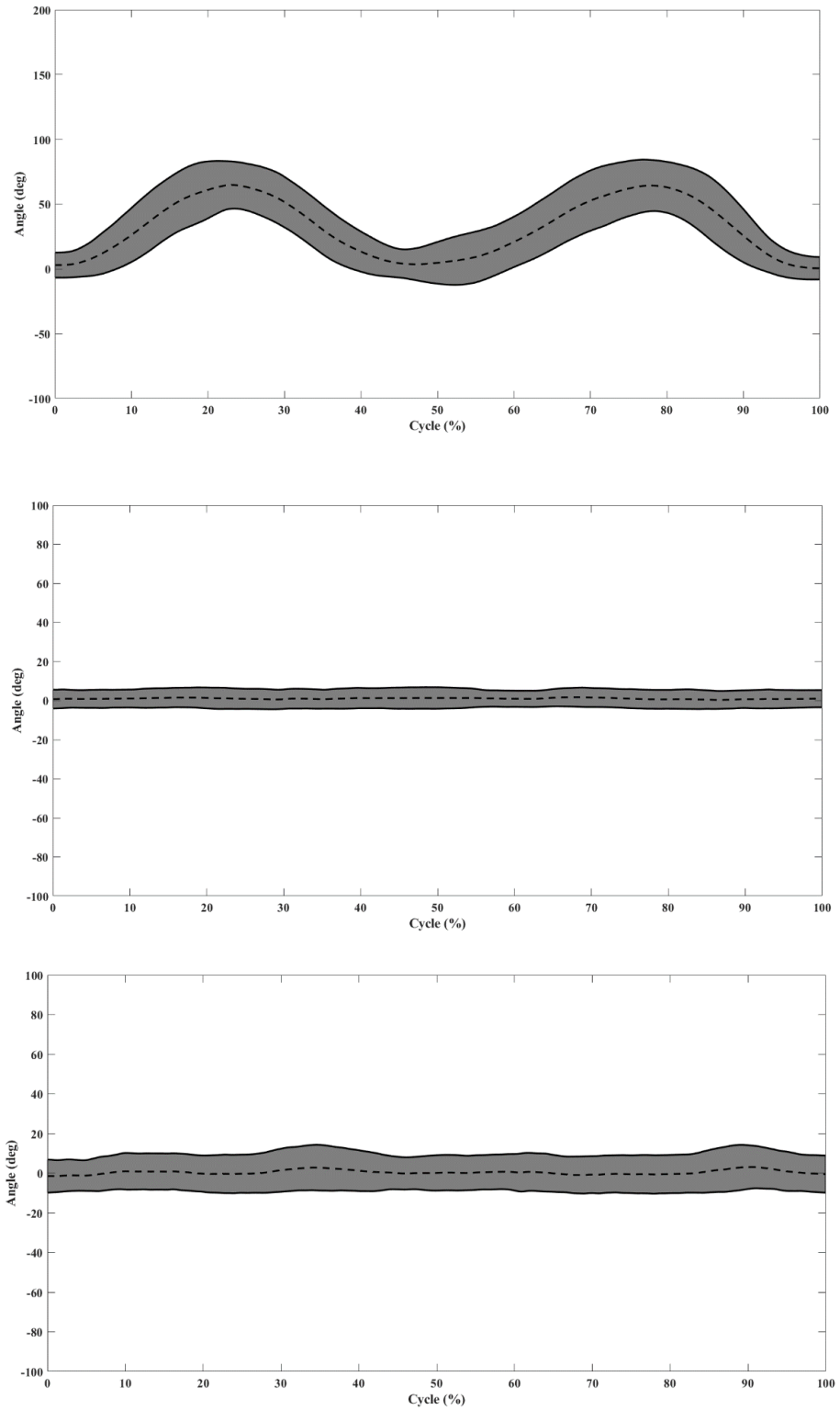

Figure 33. Hip Joint Range of Motion for Stoop Lifting

The hip flexion - extension movement has considerably higher standard deviation value compared with abduction – adduction and internal – external rotation movements of the hip joint.

3.2.3. Squat Lifting

The maximum, minimum and range of motion values of each hip joint axis are found for Squat Lifting activity and tabulated in Table 11.

The hip joint has a flexion-extension range of motion of 96.45° with maximum angle of 101.0° and minimum angle of 4.55°. The hip joint has an abduction-adduction range of motion of 2.41° with maximum angle of 2.50° and minimum angle of 0.09°. The hip joint has an internal-external rotation range of motion of 4.23° with maximum angle of 4.32° and minimum angle of 0.09°.

Table 11. Max., min., and RoM Values of Hip Joint in Squat Lifting

	Squat Lifting		
	Max	Min	RoM
Hip F-E	101.0°	4.55°	96.45°
Hip ABD-ADD	2.50°	0.09°	2.41°
Hip I-E ROT	4.32°	0.09°	4.23°

Dynamic models that were created in Visual3D for Squat Lifting are given in Figure 34.

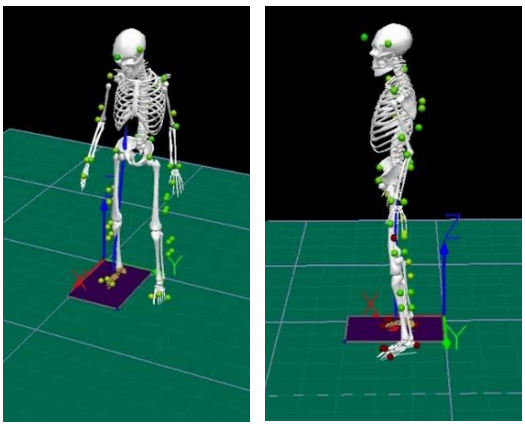

Figure 34. Dynamic Full Body Model of Squat Lifting in Visual3D

Figure 35 shows the variability of the motion through volunteers by taking account mean and standard deviation.

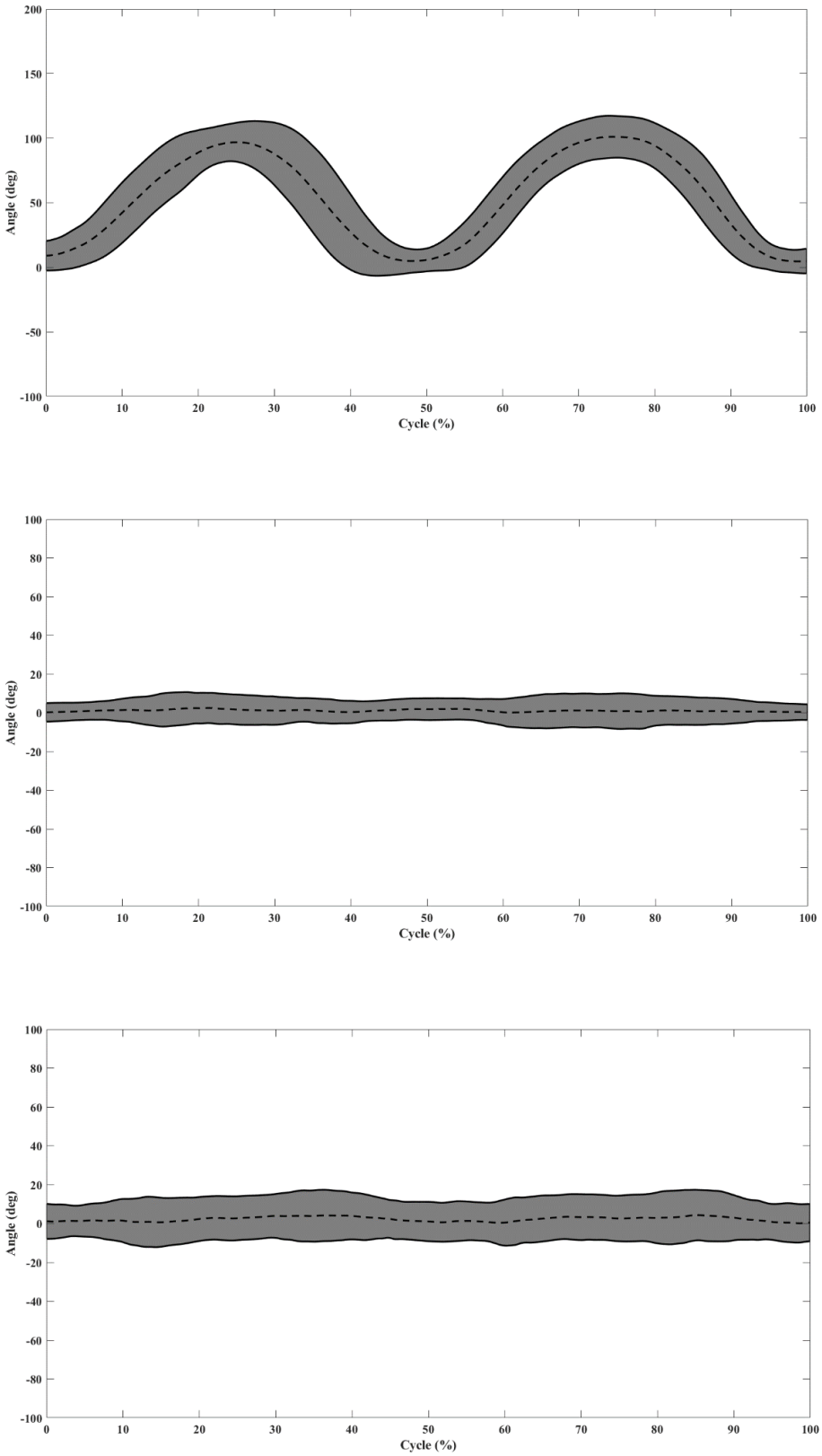

Figure 35. Hip Joint Range of Motion for Squat Lifting

The hip flexion - extension movement has considerably higher standard deviation value compared with abduction – adduction and internal – external rotation movements of the hip joint.

3.2.4. Asian Style Sitting

The maximum, minimum and range of motion values of each hip joint axis are found for Asian Style Sitting activity and tabulated in Table 13.

The hip joint has a flexion‑extension range of motion of 104.39° with maximum angle of 110.82° and minimum angle of 6.43°. The hip joint has an abduction‑adduction range of motion of 3.0° with maximum angle of 3.29° and minimum angle of 0.29°. The hip joint has an internal‑external rotation range of motion of 5.63° with maximum angle of 3.16° and minimum angle of -2.47°.

Table 1. Max., min., and RoM of Hip Joint in Asian Style Sitting

	Asian Style Sitting		
	Max	Min	RoM
Hip F-E	110.82°	6.43°	104.39°
Hip ABD-ADD	3.29°	0.29°	3.0°
Hip I-E ROT	3.16°	-2.47°	5.63°

Dynamic models that were created in Visual3D for Asian Style Sitting are given in Figure 36.

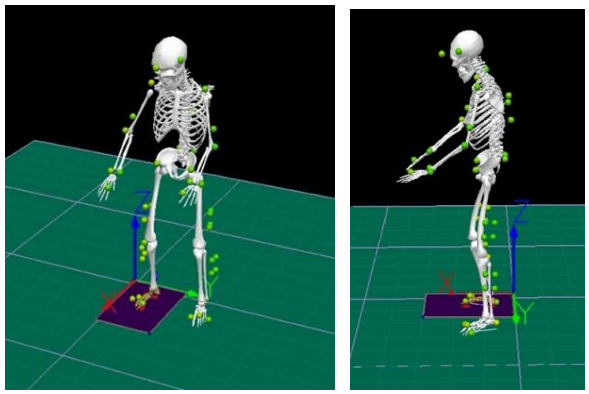

Figure 36. Dynamic Full Body Model of Asian Style Sitting in Visual3D

Figure 37 shows the variability of the motion through volunteers by taking account mean and standard deviation.

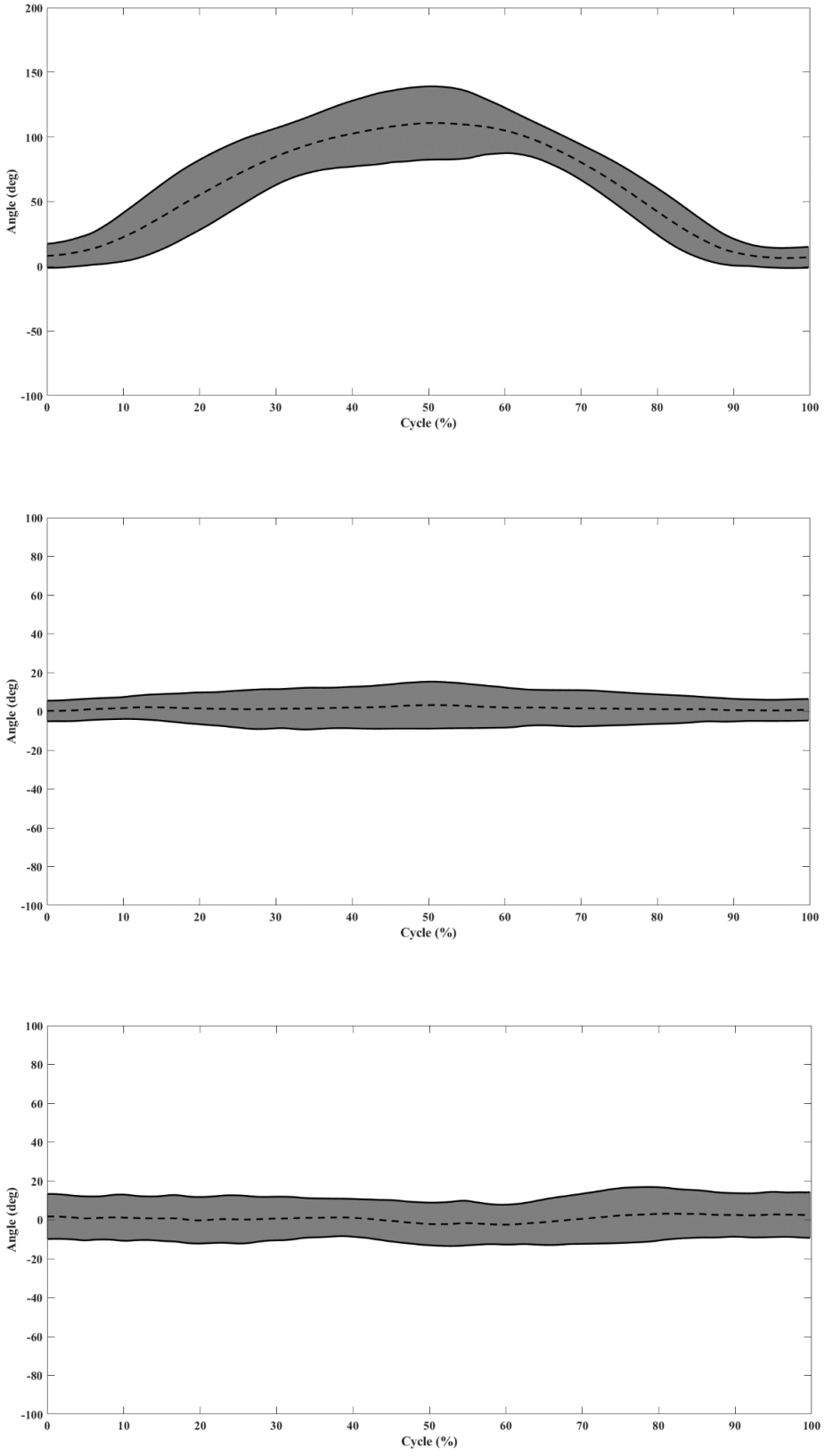

Figure 37. Hip Joint Range of Motion for Asian Style Sitting

The hip flexion - extension movement has considerably higher standard deviation value compared with abduction – adduction and internal – external rotation movements of the hip joint.

3.2.5. I'tidal to Ruku'

The maximum, minimum and range of motion values of each hip joint axis are found for I'tidal to Ruku' activity and tabulated in Table 12.

The hip joint has a flexion-extension range of motion of 54.68° with maximum angle of 57.25° and minimum angle of 2.47°. The hip joint has an abduction-adduction range of motion of 1.16° with maximum angle of 1.25° and minimum angle of 0.09°. The hip joint has an internal-external rotation range of motion of 4.38° with maximum angle of 2.18° and minimum angle of -2.20°.

Table 12. Max., min., and RoM Values of Hip Joint in I'tidal to Ruku'

	I'tidal to Ruku'		
	Max	Min	RoM
Hip F-E	57.25°	2.47°	54.68°
Hip ABD-ADD	1.25°	0.09°	1.16°
Hip I-E ROT	2.18°	-2.20°	4.38°

Dynamic models that were created in Visual3D for I'tidal to Ruku' are given in Figure 38.

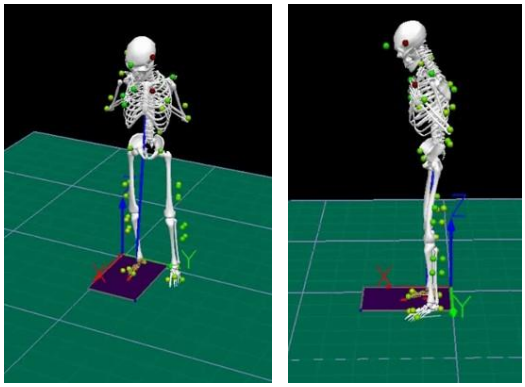

Figure 38. Dynamic Full Body Model of I'tidal to Ruku' in Visual3D

Figure 39 shows the variability of the motion through volunteers by taking account mean and standard deviation.

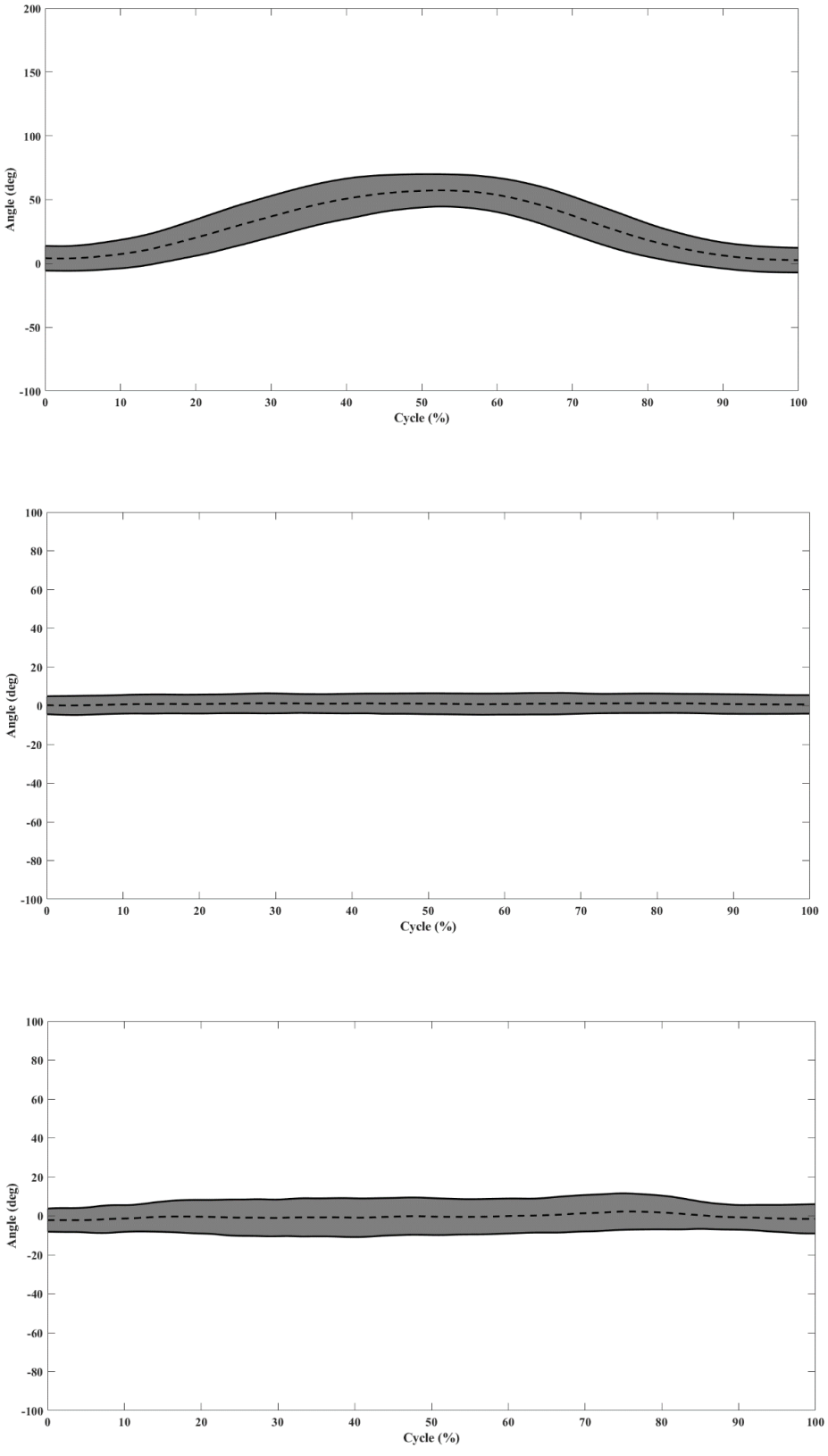

Figure 39. Hip Joint Range of Motion for I'tidal to Ruku'

The hip flexion - extension movement has considerably higher standard deviation value compared with abduction – adduction and internal – external rotation movements of the hip joint.

3.2.6. I'tidal to Sujud

The maximum, minimum and range of motion values of each hip joint axis are found for I'tidal to Sujud' activity and tabulated in Table 13.

As seen in the table, the hip joint has a flexion‑extension range of motion of 73.22° with maximum angle of 81.7° and minimum angle of 8.48°. The hip joint has an abduction‑adduction range of motion of 8.58° with maximum angle of 7.85° and minimum angle of -0.73°. The hip joint has an internal‑external rotation range of motion of 11.0° with maximum angle of 10.78° and minimum angle of -0.22°.

Table 13. Max., min., and RoM Values of Hip Joint in I'tidal to Sujud

	I'tidal to Sujud		
	Max	Min	RoM
Hip F-E	81.7°	8.48°	73.22°
Hip ABD-ADD	7.85°	-0.73°	8.58°
Hip I-E ROT	10.78°	-0.22°	11.00°

Dynamic models that were created in Visual3D for I'tidal to Sujud are given in Figure 40.

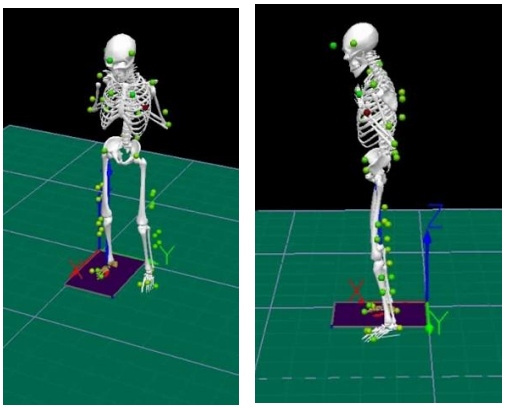

Figure 40. Dynamic Full Body Model of I'tidal to Sujud in Visual3D

Figure 41 shows the variability of the motion through volunteers by taking account mean and standard deviation.

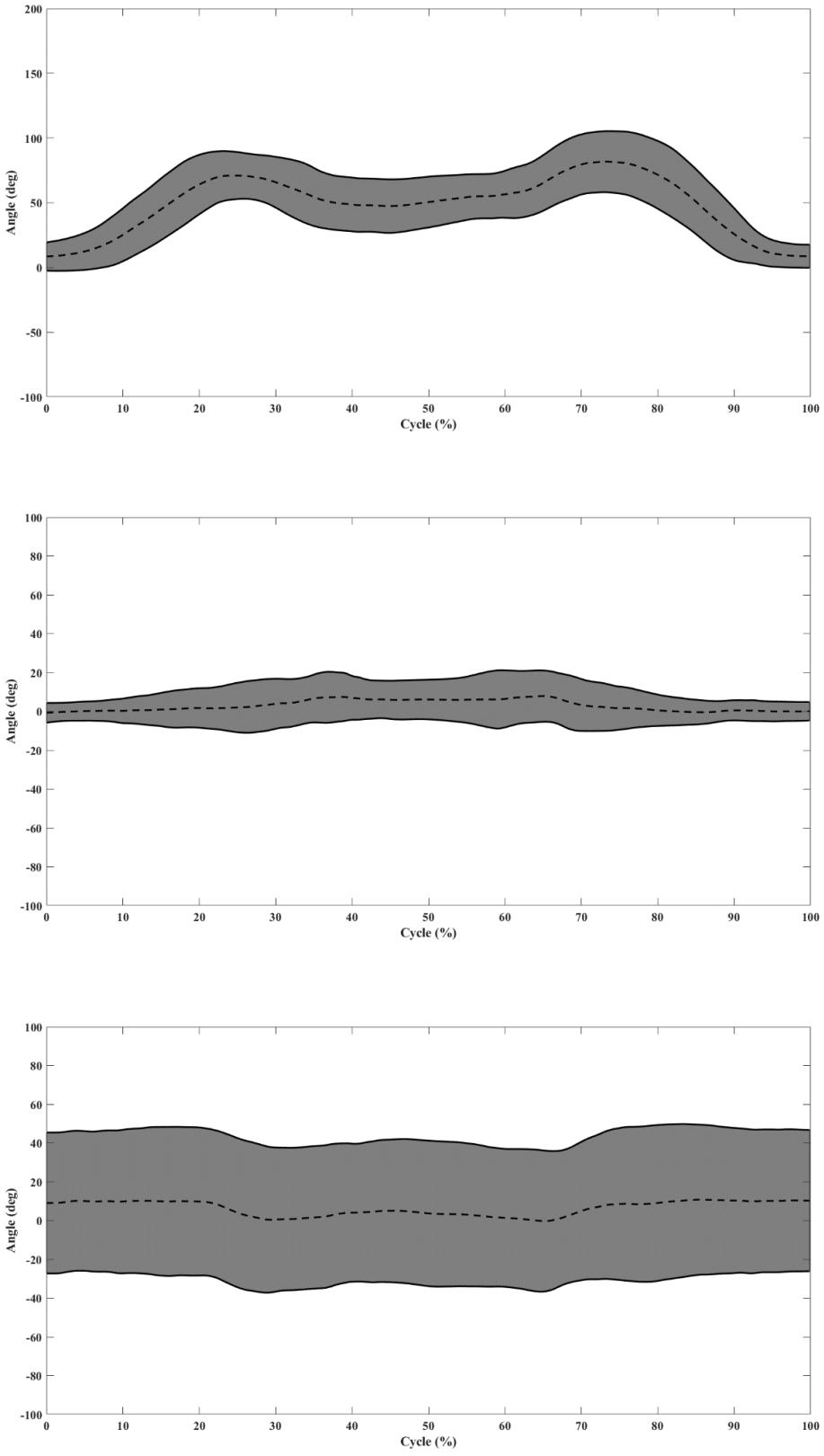

Figure 41. Hip Joint Range of Motion for I'tidal to Sujud

The hip internal-external rotation movement has considerably higher standard deviation value compared with flexion-extension and abduction-adduction and movements of the hip joint.

During the experiments, the volunteers performed the determined activities same as they do in their daily lives. Therefore, the standard deviation in a small range through the activities is expected due to unique behavior of each volunteer.

Range of motion results of each daily life activity in each relative axis is given in Figure 42 to provide an overview.

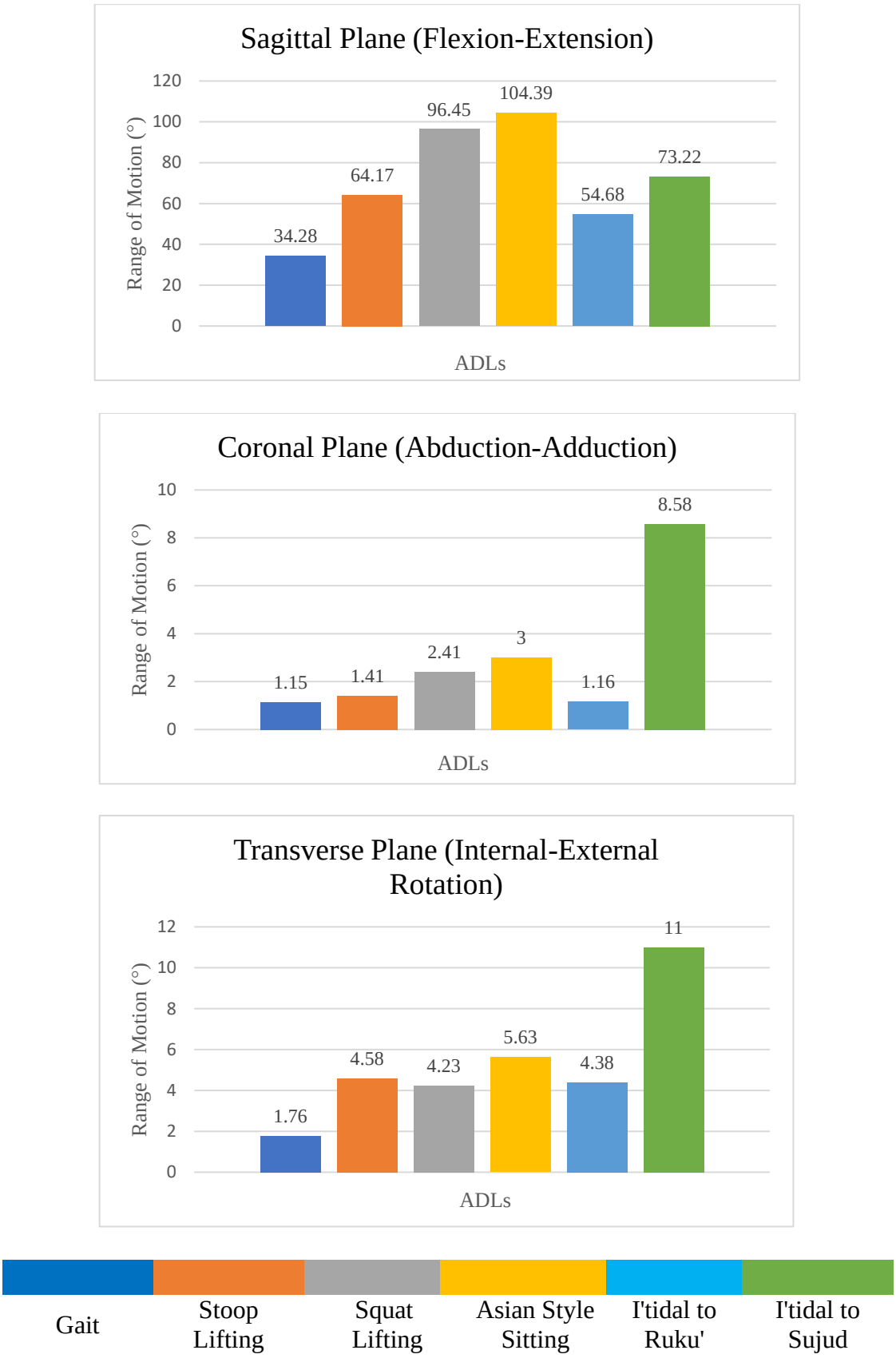

Figure 42. RoM Values of Each ADLs in Sagittal, Coronal and Transverse Plane

Asian style sitting has the highest range of motion in sagittal plane followed by the squat lifting. These activities are frequently performed during Turkish people's daily lives and due to their performing types, these activities affect the hip joint in sagittal plane the most. Gait has the lowest range of motion due to the similarity between performing walking types of the population.

I'tidal to Sujud has the highest range of motion in coronal plane while Gait and I'tidal to Ruku' have the lowest range of motion. Similarly, I'tidal to Sujud has the highest range of motion in the transverse plane while Gait has the lowest range of motion. The reason of that, Turkish people performs I'tidal to Sujud in very different ways. Also, the marker cluster might affect the performing the activity due to its rigidity.

There are many articles about hip joint kinematics in the literature. After the research, these articles were reduced to a certain number and listed in Table 1. The articles listed are intended to provide an overview on the frequently performed daily life activities to investigate hip joint kinematics. In the literature, there are a small number of studies related with the prayer activities of Muslim people. Therefore, the comparison between the literature is made between the similar activities.

The literature survey shows that the daily life activities are affecting the hip joint in sagittal plane the most.

Also, common activities between this study and the literature survey shows similar results. Squat results of the hip joint are in a similar trend with Sugano et al. (2012), Hemmerich et al. (2006) in sagittal plane. The coronal and transverse plane results similarity might be affected by the posture or performing style of the volunteer. Gait results of the hip joint is in a similar trend with Nakashima et al. (2014) in each plane. I'tidal to Sujud results of the hip joint is in a similar trend with Bowing while sitting on legs fully flexed at the knee, Zarei, Sugano et al. (2012) in each plane.

Line-of-sight problem is a critical problem for the collection of data. The line-of-sight problem has occurred the experiments frequently. Before the extrapolation methods within the QTM is utilized, the best location for the cameras is determined by feasibility studies. Although the finalized location of the cameras has the best observation sight, the line-of-sight problem still can occur due to the activity type. During the activities, the reflective markers can be blocked by the volunteer himself/herself or markers can fall from the volunteer's body. For example, L_IAS and R_IAS markers are blocked during Asian Style Sitting activity. In this situation, extrapolation methods are used to overcome the situation.

Another limit observed in the experiment is related with the marker clusters. Marker clusters contain thigh and shank markers with a group of four. The cluster is rigid material made from ABS by using 3-D printer. The rigidness of the clusters can be resistive to activities that include bending such as squat lifting, Asian Style Sitting, I'tidal to Sujud. Therefore, volunteers are asked to do the movements in a way that they feel comfortable in order to reduce this problem.

CHAPTER 4

CONCLUSION

Hip joint kinematics was investigated for daily life activities in this thesis study.

The six daily life activities were selected due to their repetitiveness and effects on the hip joint. The activities gait, stoop lifting, squat lifting, Asian style sitting and I'tidal to Ruku', I'tidal to Sujud are most common six activity that Turkish population performs in their everyday lives. Therefore, these movements have significant effect on the hip joint.

The data collection for the analysis was performed by a gold standard motion capture system Qualisys. Before the data collection, a calibration process has been completed. Thereafter, the cameras were checked to reduce line-of-sight problems. After preparation of the workspace, volunteers were prepared for the experiments. The preparation process includes measuring the anthropometric values of each volunteer by a physiotherapist to reduce mislocated marker problems. The reflective markers were placed onto the anatomical locations on the volunteer's body after measuring process was done. Once the volunteer is ready, a static calibration pose was taken. The static pose is a very crucial step for the analysis section. Each segment of the body is defined according to the static pose. After taking the static pose, additional markers were removed, and the activities were performed.

Each volunteer performed the determined activities in order. The volunteers are asked to perform the activities as they do in their daily lives. Since the aim of the project is to collect the real data of the population, the comfort of the volunteers is an important step for the healthy data collection. Each activity has been collected for a defined cycle.

The collected data is processed in QTM for the labelling of the reflective markers. After labelling the markers correctly, each activity file is exported as C3D files which contains all information about the activity to be used in inverse kinematics calculations. The C3D files were used in Visual3D software to build full body model by using static pose. The model was built by using defined marker set and template. After that, a pipeline was created to perform inverse kinematic analysis.

Inverse kinematic analysis results are obtained as tsv format for each volunteer. The calculated data was used to obtain range of motion variability through the volunteers. Therefore, statistical methods were performed on the hip joint data. The mean and standard deviation were calculated. Accordingly, the upper and lower boundaries of the range of motion for each activity is found and plotted by using MATLAB.

REFERENCES

Anang, Nurhazwani, N. Tahir, R. Jailani, H. Manaf (2016). “Analysis of Kinematic Gait Parameters in Chronic Stroke Survivors.” 2016 IEEE Symposium on Computer Applications &Amp; Industrial Electronics (ISCAIE), IEEE.

Bertec (2016) ‘Force Plate FP4060-08’, pp. 7–8.

BEST Performance Group, “Optical Motion Capture.”, (2015), Available online (2022) at: www.bestperformancegroup.com/?page_id=31

Bowman, Karl F., J. Fox, J and K. Sekiya (2010), “A Clinically Relevant Review of Hip Biomechanics.” Arthroscopy: The Journal of Arthroscopic &Amp; Related Surgery, vol. 26, no. 8, Elsevier BV, pp. 1118–29.

Cappozzo, A., Catani, F., Della Croce, U., & Leardini, A. (1995). “Position and Orientation in Space of Bones During Movement: Anatomical Frame Definition and Determination.” Clinical Biomechanics, 10(4), 171–178.

C3d.org, “Tthe 3D standard”, (2022). Available online (2022) at: www.c3d.org.

Charbonnier, Caecilia, S Chague, J. Schmid and F. Kolo (2015), “Analysis of hip range of motion in everyday life: a pilot study.” Hip international: the journal of clinical and experimental research on hip pathology and therapy vol. 25,1, pp. 82-90.

Clinicalgate, “Hip.”, (2015). Available online (2022) at: www.clinicalgate.com/hip-5.

Crossfit, “Movement About Joints, Part 5: The Hip”, (2019). Available online (2022) at: www.crossfit.com/essentials/movement-about-joints-part-5-the-hip.

Draicchio F. et al. (2010), “Global Biomechanical Evaluation During Work and Daily Life Activities.” Proceedings of the Third International Conferance on Biomedical Electronics and Devices, pp. 108-112.

Güleç, E. et al. (2009). “Anadolu insaninin antropometrik Boyutlari : 2005 Yili Türkiye AntropometrIi Anketi Genel Sonuclari”, Ankara Üniversitesi Dil ve Tarih-Coğrafya Fakültesi Dergisi, 49(2), pp. 187–201.

Hara, D., Nakashima, Y., Hamai, S., Higaki, H., Ikebe, S., Shimoto, T., Hirata, M., Kanazawa, M., Kohno, Y., Iwamoto, Y., (2014). “Kinematic Analysis of Healthy Hips during Weight-Bearing Activities by 3D-to-2D Model-to-Image Registration Technique”. BioMed Research International, 1–8. doi:10.1155/2014/457573

Hemmerich, A., Brown, H., Smith, S., Marthandam, S. S. K., & Wyss, U. P (2006). “Hip, knee, and ankle kinematics of high range of motion activities of daily living”. Journal of Orthopaedic Research, 24(4), 770–781. doi:10.1002/jor.20114

Howell, Damien. “Knee Pain Wringing Out – Gait Deviation.”, (2019). Available online (2022) at: damienhowellpt.com/knee-pain-wringing-out-gait-deviation.

Human-Motion Capture, “Electromagnetic Measurement Systems.” Accuracy of Human Motion Capture Systems for Sport Applications, (2018). Available online (2022) at: human-motioncapture.com/measurement-systems/electromagnetic-measurement-systems.

Hyodo, Kashitaro et al. (2017), “Hip, knee, and ankle kinematics during activities of daily living: a cross-sectional study.” Brazilian journal of physical therapy vol. 21,3, pp. 159-166.

Iosa, M. et al. (2018), “Assessment of Waveform Similarity in Electromyographical Clinical Gait Data: The Linear Fit Method.” J. Med. Biol. Eng. 38, 774–781.

Jonas Lindequist, and Daniel Lönnblom (2004), “Construction of a Motion Capture System.” Diva-Portal, no. ISSN 1650-2647, Report 04087.

Krigslund, R., S. Dosen, P. Popovski , J. L. Dideriksen , G. F. Pedersen and D. Farina (2013), “A Novel Technology for Motion Capture Using Passive UHF RFID Tags.” IEEE Transactions on Biomedical Engineering, vol. 60, no. 5, Institute of Electrical and Electronics Engineers (IEEE), pp. 1453–57.

Lavecchia, F., L. M. Galantucci and G. Percoco (2009), “A Simple Photogrammetric System for Automatic Capture and Measurement of Facial Soft Tissues During Movement.” Innovative Developments in Design and Manufacturing, CRC Press.

Liang, P., Kwong, W.H., Sidarta, A. et al. (2020). “An Asian-centric human movement database capturing activities of daily living”. Sci Data 7, 290. https://doi.org/10.1038/s41597-020-00627-7

Liu, Q., Yang, D., Hao, W., & Wei, Y. (2018). Research on Kinematic Modeling and Analysis Methods of UR Robot. 2018 IEEE 4th Information Technology and Mechatronics Engineering Conference (ITOEC). doi:10.1109/itoec.2018.8740681

“Magnetic Motion Capture Systems.” Polhemus Liberty, https://polhemus.com/motion-tracking/all-trackers/liberty.

Meldrum, D., Shouldice, C., Conroy, R., Jones, K. & Forward, M. (2014). “Test-retest reliability of three dimensional gait analysis: Including a novel approach to visualising agreement of gait cycle waveforms with Bland and Altman plots”. Gait Posture 39, 265–271.

Mihcin, Senay, et al. (2020), “Wearable Motion Capture System Evaluation for Biomechanical Studies for Hip Joints.” Journal of Biomechanical Engineering, Crossref, doi:10.1115/1.4049199.

Miki, H., Kyo, T., & Sugano, N. (2012). “Anatomical Hip Range of Motion After Implantation During Total Hip Arthroplasty With a Large Change in Pelvic Inclination”. The Journal of Arthroplasty, 27(9), 1641–1650.e1. doi:10.1016/j.arth.2012.03.002

Norkin C, C, White, D.J. (2016). “Measurement of joint Motion: A Guide to Ganiometry”. 5th Edition. USA: F.A.Davis Company.

Novaorthospine, “Hip Anatomy”. Available online (2022) at: www.novaorthospine.com/specialties/hip/hip_anatomy.

Ocran, Edwin. “Hip Joint.”, (2022). Available online (2022) at: www.kenhub.com/en/library/anatomy/hip-joint.

Perry, J., J. M. Burnfield (2010), “Gait Analysis: Normal and Pathological Function”, ISBN:978- 1556427664, Slack Incorporated

Qualisys, “Miqus.”, (2014) www.qualisys.com/cameras/miqus. Available at: https://www.qualisys.com/cameras/miqus/#!#tech-specs (Accessed: 27 February 2021).

Qualisys, “Motion Capture – Mocap.”, (2022). Available online (2022) at: https://www.qualisys.com/.

Qualisys, “Small carbon fiber calibration kit.”, (2018) www.qualisys.com/accessories/calibration-kits/small-carbon-fibre-calibration-kit/. Available at: (Accessed: 27 February 2021).

Qualisys, “Super-spherical markers.”, (2014) www.qualisys.com/accessories/markers/super-spherical-markers/. Available at: (Accessed: 27 February 2021).

Sataloff, Robert T., Johns, Michael M., Kost, Karen M. (2011). QTM User Manual. Sweden: Qualisys AB.

Schepers, M., Giuberti, M. and Bellusci, G. (2018). ‘Xsens MVN: Consistent Tracking of Human Motion Using Inertial Sensing’, Xsens Technologies, (March), pp. 1–8.

Sint Jan S. V. (2007). “Color Atlas of Skeletal Landmark Definitions: Guidelines for Reproducible Manual and Virtual Palpations”. Churchill Livingstone/Elsevier.

Smartsuit-Pro Tech specs (2020). Available at: https://www.rokoko.com/products/smartsuit-pro/tech-specs (Accessed: 27 February 2021).

Sugano, N., Tsuda, K., Miki, H., Takao, M., Suzuki, N., & Nakamura, N. (2012). “Dynamic Measurements of Hip Movement in Deep Bending Activities After Total Hip Arthroplasty Using a 4-Dimensional Motion Analysis System”. The Journal of Arthroplasty, 27(8), 1562–1568. doi:10.1016/j.arth.2012.01.029

Şenay Mihçin, Ahmet Mert Sahin, Mehmet Yılmaz, Alican Tuncay Alpkaya, Merve Tuna, Nuray Korkmaz Can, … Aliye. (2023, 31 Ocak). “Database Covering the Previously Excluded Daily Life Activities.” doi:10.48623/aperta.252060

Torricelli, Diego, et al. (2018), “A Subject-Specific Kinematic Model to Predict Human Motion in Exoskeleton-Assisted Gait.” Frontiers in Neurorobotics, vol. 12. Crossref, doi:10.3389/fnbot.2018.00018.

Tozkoparan, K. E. and O Karaduman (2022), “Spor Biyomekaniğinde Performans Analizi Için Hareket Yakalama Teknolojisi Uygulamaları.”, Istanbul University-DergiPark

Tracklab, “C-Motion Visual 3D.” (2020), Available online (2022) at: www.tracklab.com.au/products/brands/c-motion/c-motion-visual-3d.

Ziegler, Jakob, et al. (2020). “Simultaneous Identification of Human Body Model Parameters and Gait Trajectory from 3D Motion Capture Data.” Medical Engineering & Physics, vol. 84, pp. 193–202., https://doi.org/10.1016/j.medengphy.2020.08.009.

Wu, Ge, et al. (2002) “ISB Recommendation on Definitions of Joint Coordinate System of Various Joints for the Reporting of Human Joint Motion—Part I: Ankle, Hip, and Spine.” Journal of Biomechanics, vol. 35, no. 4, pp. 543–548., https://doi.org/10.1016/s0021-9290(01)00222-6.